

## Article

# Drying Time, Energy and Exergy Efficiency Prediction of Corn (*Zea mays* L.) at a Convective-Infrared-Rotary Dryer: Approach by an Artificial Neural Network

Yousef Abbaspour-Gilandeh <sup>1,\*</sup>, Safoura Zadhosein <sup>1</sup>, Mohammad Kaveh <sup>2</sup>, Mariusz Szymanek <sup>3,\*</sup>, Sahar Hassannejad <sup>4</sup> and Krystyna Wojciechowska <sup>5</sup>

- <sup>1</sup> Department of Biosystems Engineering, College of Agriculture and Natural Resources, University of Mohaghegh Ardabili, Ardabil 56199-11367, Iran; safoorazadhosein@yahoo.co.uk
- <sup>2</sup> Department of Petroleum Engineering, College of Engineering, Knowledge University, Erbil 44001, Iraq; sirwankaweh@gmail.com
- <sup>3</sup> Department of Agricultural, Forest and Transport Machinery, University of Life Sciences in Lublin, Głęboka 28, 20-612 Lublin, Poland
- <sup>4</sup> Department of Medical Laboratory Science, College of Science, Knowledge University, Erbil 44001, Iraq; sahar.hassannejad@knu.edu.iq
- <sup>5</sup> Department of Strategy and Business Planning, Faculty of Management, Lublin University of Technology, 20-618 Lublin, Poland; k.wojciechowska@pollub.pl
- \* Correspondence: abbaspour@uma.ac.ir (Y.A.-G.); mariusz.szymanek@up.lublin.pl (M.S.)

**Abstract:** Energy consumption in the drying industry has made drying an energy-intensive operation. In this study, the drying time, quality properties (color, shrinkage, water activity and rehydration ratio), specific energy consumption (S.E.C), thermal, energy and exergy efficiency of corn drying using a hybrid dryer convective-infrared-rotary (CV-IR-D) were analyzed. In addition, the energy parameters and exergy efficiency of corn were predicted using the artificial neural network (ANN) technique. The experiments were conducted at three rotary rotation speeds of 4, 8 and 12 rpm, drying temperatures of 45, 55 and 65 °C, and infrared power of 0.25, 0.5 and 0.75 kW. By increasing drying temperature, infrared power and rotary rotation speed, the drying time, S.E.C and water activity decreased while the  $D_{eff}$ , energy, thermal and exergy efficiency increased. In addition, the highest values of rehydration ratio and redness ( $a^*$ ) and the lowest values of shrinkage, brightness ( $L^*$ ), yellowness ( $b^*$ ) and color changes ( $\Delta E$ ) were obtained at an infrared power of 0.5 kW, air temperature of 55 °C and rotation speed of 8 rpm. The range of changes in S.E.C, energy, thermal and exergy efficiency during the corn drying process was 5.05–28.15 MJ/kg, 3.26–29.29%, 5.5–32.33% and 21.22–55.35%. The prediction results using ANNs showed that the R for the drying time, S.E.C, thermal, energy and exergy data were 0.9938, 0.9906, 0.9965, 0.9874 and 0.9893, respectively, indicating a successful prediction.

**Keywords:** corn; energy efficiency; exergy efficiency color; rehydration ratio

Academic Editor: Azharul Karim

Received: 27 December 2024

Revised: 21 January 2025

Accepted: 30 January 2025

Published: 3 February 2025

**Citation:** Abbaspour-Gilandeh, Y.; Zadhosein, S.; Kaveh, M.; Szymanek, M.; Hassannejad, S.; Wojciechowska, K. Drying Time, Energy and Exergy Efficiency Prediction of Corn (*Zea mays* L.) at a Convective-Infrared-Rotary Dryer: Approach by an Artificial Neural Network. *Energies* **2025**, *18*, 696. <https://doi.org/10.3390/en18030696>

**Copyright:** © 2025 by the authors. Licensee MDPI, Basel, Switzerland. This article is an open access article distributed under the terms and conditions of the Creative Commons Attribution (CC BY) license (<https://creativecommons.org/licenses/by/4.0/>).

## 1. Introduction

Corn, scientifically known as *Zea mays* L., is a member of the gramineae family and is one of the most productive cereals in the world. Corn ranks third in terms of cultivated area after rice and wheat [1]. Corn has many uses in human, livestock, poultry and industrial nutrition [2] and is highly adaptable to growing in various climatic conditions. Corn

contains carbohydrates, protein, iron, vitamin B and minerals [3]. Freshly harvested corn grain has a high moisture level of 20 to 30% on a wet basis (wb) [4]. Considering the applications of corn in various fields, one of the methods of processing it in order to make this product better and more use of it is drying it in order to maintain its quality and shelf life by reducing or eliminating the moisture in corn, which is the main factor in its spoilage after harvest [5]. During the drying process, the moisture content of the product is reduced through simultaneous mass and heat transfer, which prevents microbial activity, reduces weight and costs, makes transportation easier and increases the shelf life [6].

Various reports have documented the effects of hot air [4,7], fluidized bed [8,9], infrared power [10–12] and microwave radiation [13–15] on corn drying. A review of the reports revealed that efforts have been made to find better energy-efficient drying techniques to improve corn quality. Each of the reported drying methods for corn has its own inherent advantages and disadvantages.

The first and oldest method of drying was by sunlight, and today this traditional, environmentally friendly method is still used in some areas, but due to the long time required and dust and insect attacks during the drying process, the quality of corn decreases [16,17]. The most common method of drying products is to use hot air flow, where hot air flows over the surface of the product, and over time, the speed of the drying process and product quality decreases and energy consumption increases [7]. Therefore, the use of combined methods such as infrared waves has always been considered due to the penetration of waves into the product, increasing the collision speed of water molecules, generating heat and stimulating moisture out of the product [18].

On the other hand, rotary dryers are one of the most modern techniques for drying grain materials [18,19], medicinal plants [20], fruits [21,22] and seafood [16] that have been successfully used. This type of dryer consists of a cylindrical chamber with the ability to rotate around its axis [23]. Therefore, the rotary capability in dryers, along with other prominent features of other dryers, such as infrared power and hot air, in the form of a hybrid dryer, dries the entire product uniformly (due to the forward movement of the product along the cylinder and the adjustable rotary rotation speed) and has higher capabilities than other dryers [20].

In recent years, several studies have been conducted on the analysis of the kinetics and qualitative and thermal properties of various types of agricultural products in a combined rotary dryer with other systems. Through these studies, the thermal behavior of the dryer can be determined in terms of heat generation and the effect of various parameters on the performance of the dryer. For example, the thermal and qualitative behavior of Kaffir lime leaf and red chili pepper in the microwave-rotary method has been comprehensively discussed by Pradechboon et al. [24,25]. In addition, Ghasemkhani et al. [26] conducted the qualitative properties of apples in a rotating-tray convective dryer system. Kaveh et al. [19] conducted a similar study for peas considering the effects of air temperature and rotary speed. Basseyy et al. [22] also investigated the color and resorption coefficient analyses and evaluation of the bioactive properties of red dragon fruit using a combined infrared-rotary system. Energy consumption, thermal efficiency and bioactive properties of flaxseeds were determined by Alshehri et al. [18] using the infrared-rotary technique to determine the drying potential. Jayaram et al. [27] proposed a new method based on a solar collector for a combined rotary-hot air dryer in which specific energy consumption, dryer efficiency and specific moisture extraction rate were also considered. Balakrishnan et al. [20] studied the effect of design parameters on the drying performance of turmeric rhizomes in a rotary method. The energy efficiency and kinetics of rice drying in a rotary fluidized-bed dryer were reviewed by Singh et al. [28]. Kaveh et al. [23] investigated the effect of various parameters on the energy and exergy of rice drying in an infrared-rotary method. They also performed an optimization based on the effect of rotary speed

and infrared power on the parameters. A novel approach using artificial neural networks was used to predict the moisture content of shrimp in a rotary infrared dryer by Al-Hilphy et al. [16].

Since conventional methods such as statistical methods based on first principles for process prediction are time-consuming and the accuracy of the results obtained from them is not satisfactory, artificial neural networks are used because they have the power to provide the necessary accuracy and speed for predicting the drying process [29]. The simplest and most common type of neural network that has been used in many engineering sciences, including the present research, is the multilayer perceptron (MLP) neural network [30]. This neural network is used to solve nonlinear problems. The MLP network is a set of basic neurons that are placed in three layers [31]. These three layers are known as the input, hidden and output layers [32]. The artificial neural network (ANN) method has been used to model and optimize the drying process of various agricultural products including garlic [33], mint [34], apple [35], *Phyllanthus emblica* [36] and carrot [37]. The results of these studies showed that laboratory data can be well fitted by the artificial neural network.

All the measures taken to provide a new method (CV-IR-D combined method) for drying corn in the drying process may be a solution to minimize drying time and specific energy consumption and improve the qualitative and visual properties of dried corn. On the other hand, considering the initial studies on the corn drying process in different dryers, the need for changes and optimization in the agricultural product processing industry equipment to improve the qualitative properties in the drying process is felt more. Therefore, the purpose of this research is to determine the effect of different drying conditions on the time and S.E.C of the drying process, evaluate the energy, thermal and exergy efficiency and determine the qualitative characteristics (color, shrinkage, water activity and rehydration ratio) in order to achieve the best drying conditions for corn in the dryer. In addition, another objective of this study is to use ANNs to provide the best topology and optimal transfer function for predicting drying time, energy parameters and exergy efficiency.

## 2. Materials and Methods

### 2.1. Corn Preparation

In this study, freshly harvested corn was obtained from a farm in the city of Ardabil (Ardabil, Iran). After removing broken kernels and foreign matter from the samples, the AOAC standard was used to determine the initial moisture content [38]. In this way, 20 g corn samples were placed in an oven (Memmert, UFB500, Schwabach, Germany) at 105 °C for 24 hours until the weight of the samples did not change. The initial moisture content of the corn samples was 26% on a dry basis (d.b).

### 2.2. Drying Device

In this study, a combined convective-infrared-rotary cylinder (CV-IR-D) dryer from the Biosystems Engineering Department of Mohaghegh Ardabili University was used (Figure 1). The combined dryer consists of three sections (a hot air, infrared and rotary cylinder). The hot air section contains a centrifugal blower, 3 elements, an inverter, thermostat and a K-type thermocouple. The infrared section contains 4 infrared lamps (250-watt) with a distance of 10 cm from the rotating cylinder. The rotating cylinder section contains two rollers at the beginning and end, an inverter, gearbox and a cylindrical cylinder with a diameter of 36 cm and a length of 90 cm (more details in Kaveh et al. [23]).

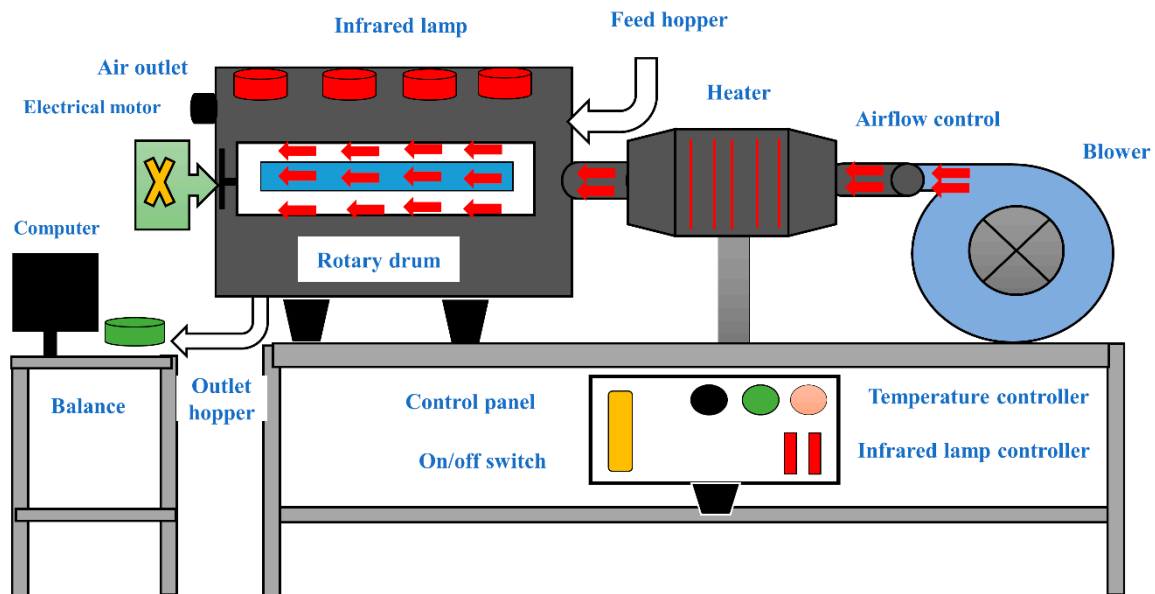


Figure 1. Schematic diagram of a convective-infrared-rotary drum (CV-IR-D) dryer.

The drying operation of corn grains is carried out inside the drying cylinder. The drying cylinder is mounted on the central tube of the cylinder by two bearings. The air flow of the dryer is introduced into the electric heater using a blower and is heated to the specified temperature and then enters the drying cylinder. During the drying operation, the samples were weighed every ten minutes using a digital scale (GF-600; Japan,  $\pm 0.001$  g) with an accuracy of  $\pm 0.1$  g, which allowed the grain moisture to be calculated at different times according to the initial moisture content of the corn grains. The 200 g samples were dried to a moisture content of 13% on a dry basis. The experiments were conducted at three temperature levels (45, 55 and 65 °C), three infrared power levels (0.25, 0.5 and 0.75 kW) and three drum rotation speed levels (4, 8 and 12 rpm) and a constant air speed of 1 m/s in three replicates.

### 2.3. Effective Moisture Diffusion

Fick's law is used to calculate the  $D_{\text{eff}}$ , which is shown in Equation (1) [11,39]:

$$MR = \frac{M_t - M_e}{M_b - M_e} = \frac{6}{\pi^2} \sum_{n=1}^{\infty} \frac{1}{2n^2} \exp\left(-n^2 \pi^2 \frac{D_{\text{eff}} t}{r_e^2}\right) \quad (1)$$

The  $D_{\text{eff}}$  is obtained by calculating the slope of Equation (2).

$$MR = \left(\frac{6}{\pi^2}\right) \exp\left(-\frac{\pi^2 D_{\text{eff}} t}{r_e^2}\right) \quad (2)$$

The  $D_{\text{eff}}$  is usually determined by plotting experimental drying data in terms of the natural logarithm of the moisture content versus time. Once the value versus time graph is plotted, the slope of the resulting line is inserted into Equation (3) to obtain the  $D_{\text{eff}}$  [15].

$$K_1 = \left(\frac{D_{\text{eff}} \pi^2}{r_e^2}\right) \quad (3)$$

#### 2.4. Measurement of the S.E.C, Energy and Thermal Efficiency

In this study, the energy supply sources in each of the sections of the CV-IR-D hybrid dryer play a role in the S.E.C. The S.E.C of the convective section can be calculated through thermal energy (Equation (4)) [40] and mechanical energy (Equation (5)) [41], infrared energy (Equation (6)) [42] and rotary energy (Equation (7)) [18]. Finally, the S.E.C of the CV-IR-D hybrid dryer is estimated from Equation (8).

$$EU_{ter} = (Av.\rho_a.C_a.\Delta T).3600 \quad (4)$$

$$EU_{mec} = (M_{air}.t.\Delta P) \quad (5)$$

$$EU_{IR} = (K.t).3600 \quad (6)$$

$$EU_D = 2.6 \times (Y.T) \quad (7)$$

$$SEC = \frac{EU_{ter} + EU_{mec} + EU_{IR} + EU_D}{M_w} \quad (8)$$

According to the analysis of El-Mesery et al. [33], the thermal efficiency during the drying of corn by CV-IR-D can be calculated using Equation (9).

$$TE = \frac{D_w Ah_{fg} (M_i - M_o)}{3600 D_i (100 - M_o)} \quad (9)$$

The energy efficiency of the energy balance equation in the first law of thermodynamics is determined as Equation (10) according to the method of Kumar et al. [6] and Lemus-Mondaca et al. [40].

$$\eta_e = \frac{Q_w}{EU} = \frac{h_{fg} M_w}{EU} \quad (10)$$

On the other hand, Equations (11) and (12) were used to calculate the volume of water removed from the product and the latent heat of vaporization, respectively [33,40].

$$m_w = \frac{m_o (X_{wo} - X_{wf})}{100 - X_{wf}} \quad (11)$$

$$h_{fg} = \begin{cases} 2.503 \times 10^6 - 2.386 \times 10^3 (T_{abs} - 273.16) & \{ 273.16 \leq T_{abs} \leq 338.72 \\ (7.33 \times 10^{12} - 1.6 \times 10^7 T_{abs}^2)^{0.5} & \{ 338.72 \leq T_{abs} \leq 533.16 \end{cases} \quad (12)$$

#### 2.5. Measurement of the Exergy Efficiency

In order to determine the exergy efficiency analysis, first the exergy balance was investigated based on the second law of thermodynamics using the following equations [43–45].

$$\sum EX_{in} = \sum EX_{out} \quad (13)$$

$$\sum EX_{in} = \sum EX_{out} - \sum EX_{dest} \quad (14)$$

Then, the input and output exergy of corn drying for the CV-IR-D closed system were estimated using Equations (15) and (16) [46].

$$\sum EX_{in} = m_{in} [h_{in} - T_0 s_{in}] \quad (15)$$

$$\sum EX_{out} = m_{out} [h_{out} - T_0 s_{out}] \quad (16)$$

In addition, the exergy loss and exergy destruction were determined using Equations (17) and (18), respectively [47,48].

$$EX_{loss} = \left(1 - \frac{T_0}{T}\right) \times Q_{loss} \quad (17)$$

$$EX_{dest} = S_{gen} T_0 \quad (18)$$

Finally, the exergy efficiency was calculated from Equation (19) [49].

$$\eta_{ex} = 1 - \frac{EX_{dest}}{EX_{in}} \times 100 \quad (19)$$

## 2.6. Qualitative Properties Investigation

### 2.6.1. Water Activity

The AW meter (Novasina, Lachen, Switzerland) was used to measure water activity. The sample was placed inside the special plate of the device and after 10 minutes the water activity level was determined on the device display.

### 2.6.2. Measurement of the Color Parameters

The color of the corn kernels was measured before and after drying using a colorimeter (HP-200, China). After the device measured the parameters  $L^*$ ,  $a^*$  and  $b^*$ , the overall color change  $\Delta E$  was calculated from the following equation [35]:

$$\Delta E = \sqrt{(\Delta L^*)^2 + (\Delta a^*)^2 + (\Delta b^*)^2} \quad (20)$$

### 2.6.3. Rehydration Ratio (RR)

This property indicates the extent to which the samples, which have lost their moisture during the drying process, have the ability to absorb water, because the drying process can affect the extent of this ability. For this purpose, the dried samples were first weighed ( $W_d$ ) and then, according to the procedure of Bassey et al. [22] (with minor modifications), the samples were immersed in distilled water at a temperature of 25 °C and at a ratio of 1:10 and were removed from the distilled water after 2 hours. After that, their weight ( $W_r$ ) was measured and finally the RR rate was obtained through the following equation [39]:

$$RR = \frac{W_r}{W_d} \quad (21)$$

#### 2.6.4. Measurement of the Shrinkage

To measure the shrinkage rate according to the method of Ghasemkhani et al. [21], the sample was poured into a certain volume of toluene in a graduated cylinder and the displaced volume was measured. For this purpose, 5 g of the sample was selected before and after drying and its volume was measured. The ratio of the volume of dried corn to the initial volume of corn is equal to the degree of shrinkage [8].

#### 2.7. Artificial Neural Networks

In this study, an artificial neural network (feed forward backpropagation) with the Levenberg–Marquardt optimization algorithm was used to predict the drying time, S.E.C, thermal, energy and exergy efficiency of the corn samples. The type of network designed was a multilayer perceptron (MLP) in which the input layer consisted of three neurons (infrared power, drying temperature and rotation speed) and the output layer consisted of one neuron (drying time, S.E.C, thermal, energy and exergy efficiency). The structure of this multilayer network is shown in Figure 2. Optimization of the neural network structure was carried out by examining different topologies and also by evaluating the difference between the outputs of the ANNs and the experimental data. To optimize the structure of the ANNs, various network parameters such as the number of hidden layers and the number of neurons in each hidden layer (by trial and error method) were evaluated. In order to find a suitable topology for the corn drying problem, one/two hidden layers with 2 to 20 neurons and 800 learning cycles were used. In the hidden layer neurons, three threshold functions of tangent sigmoid (Tan), logarithmic (Log) and linear (Pur) were used. Matlab R2019a software was used to design and test the ANN.

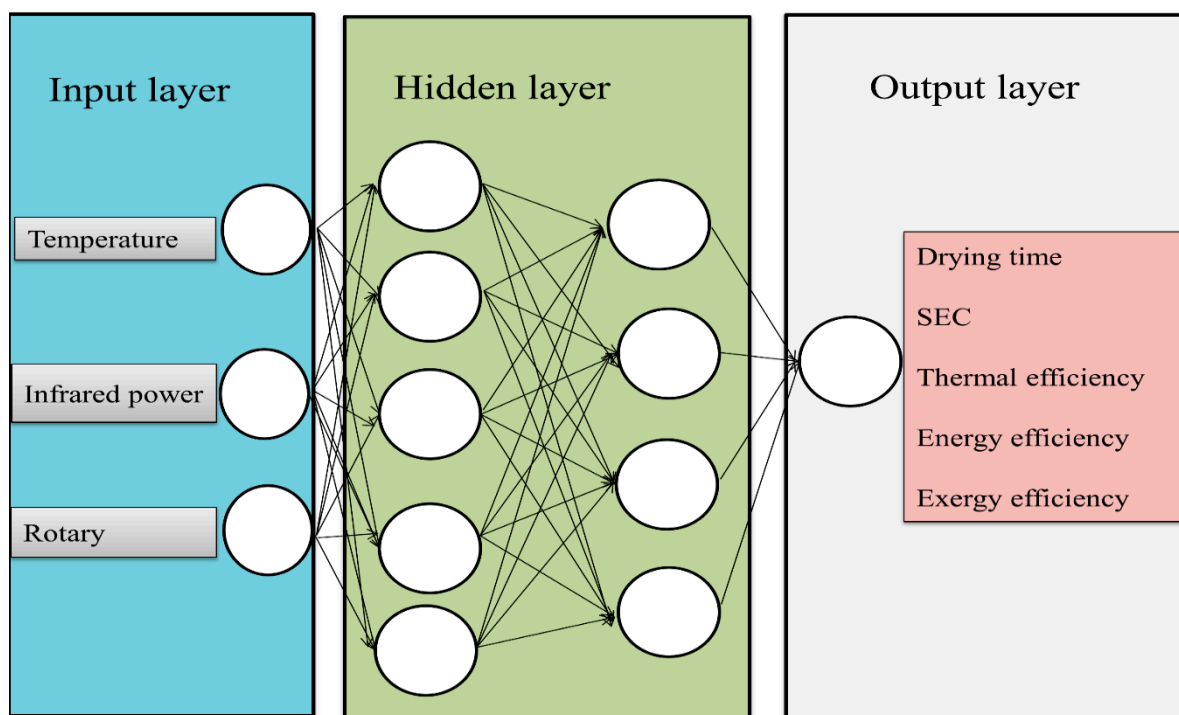


**Figure 2.** Configuration of ANN model for all parameters.

The total number of input patterns of the neural network for each of the output parameters was 81 patterns, which were first normalized and then randomly divided into three parts (training, validation and testing). The data used for training included 70% of the data and of the remaining data, 15% was used for validation and 15% for testing the network [50]. The maximum number of iterations required in the network learning

process was considered to be 500. Entering data in raw form reduces the speed and accuracy of ANNs, therefore the input data to the network must be normalized. If this step is not performed, the network will not converge during the training phase and the desired results will not be produced. Therefore, all data (input and output) were standardized and normalized between 0 and 1 using the method of Camilo et al. [51] and Equation (5).

$$X_{normal} = \frac{x_i - x_{min}}{x_{max} - x_{min}} \quad (22)$$

To find a network with a suitable architecture using training algorithms, the coefficient of determination (R) and mean square error (MSE) criteria were used. First, the values of (R) and MSE in each of the created networks were examined, which were estimated from Equations (23) and (24), and finally the network with the highest R<sup>2</sup> and the lowest MSE was accepted [52].

$$R^2 = \sqrt{1 - \frac{\sum_{i=1}^n (O_i - T_i)^2}{\sum_{i=1}^n (O_i - T_m)^2}} \quad (23)$$

$$MSE = \frac{\sum_{i=1}^n (O_i - T_i)^2}{N} \quad (24)$$

### 2.8. Statistical Analysis

In this study, data analysis was performed using SPSS software version 21, means were compared at a 5% probability level using Duncan's test, and graphs were drawn using Excel software.

## 3. Results

### 3.1. Drying Time

Figure 3 shows the effect of different treatments on the drying time of the corn samples. In this study, the drying time of corn by CV-IR-D ranged from 70 to 440 minutes, which was less than corn dried by infrared dryer [12], hot air and microwave-hot air [15]. According to the results of analysis of variance, the effect of the main treatments and interaction infrared-air temperature on drying time was significant ( $p < 0.01$ –Table 1). Figure 3 shows that increasing the infrared power treatments, drying temperature and rotation speed reduced the drying time of the samples ( $p < 0.05$ ) because the cell walls were damaged and as a result, more water was released from the tissue. In addition, by increasing the lamp power from 0.25 to 0.75 kW, the temperature from 45 to 65 °C and the rotary rotation speed from 4 to 12 rpm due to the increase in energy transferred to the samples, the drying time decreased by 84.09%. As Basseyy et al. [22] concluded, increasing the rotation speed and infrared power caused the drying time of red dragon fruit to decrease due to the increase in the moisture release rate. On the other hand, according to Figure 3, drying in treatments with lower power, temperature and rotation speed has a higher drying time (440 minutes) than other treatments. Possibly due to the damage of the surface pores and capillary tubes present on the surface of the corn, the corn surface became hard and moisture was difficult to remove from the samples and the drying time was prolonged. Wilson et al. [10] showed that increasing the infrared power caused a reduction of

approximately 70% in the drying time of corn. They attributed this to the easier migration of moisture from the inner to the surrounding areas.

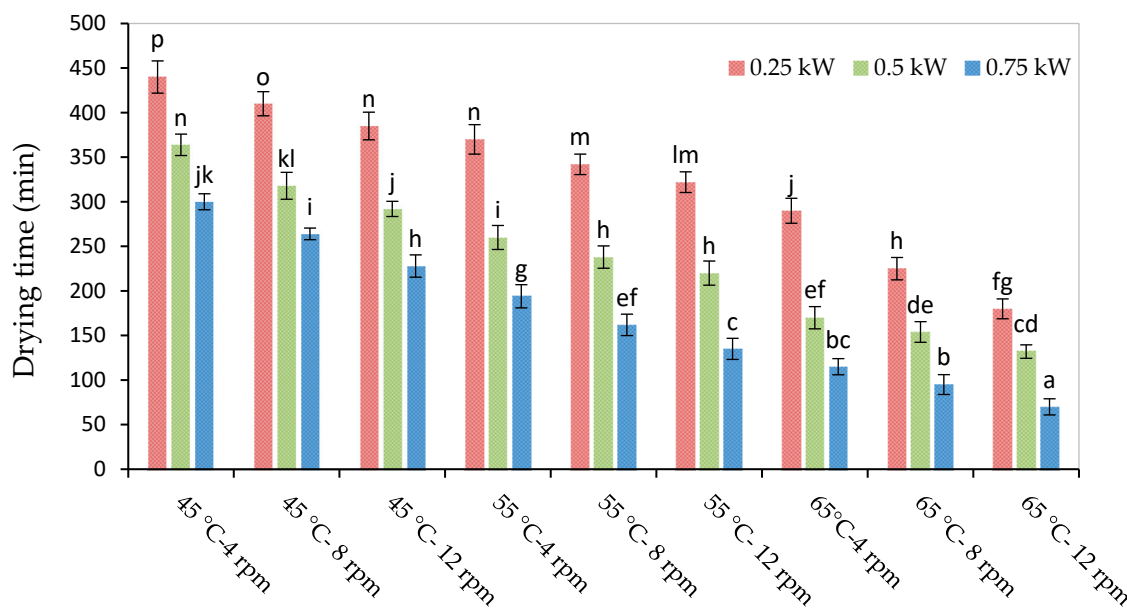


**Figure 3.** Effects of different drying conditions on drying time. Different letters in the columns have a significant difference at the 1% probability level. Similar letters in each column indicate the absence of significant differences based on Duncan’s test at the 5% probability level.

**Table 1.** ANOVA results of drying time, S.E.C, energy efficiency, thermal efficiency and exergy efficiency under different infrared power, air temperature and rotary rotation speed.

Parameter	df	Drying Time		S.E.C		Energy Efficiency		Thermal Efficiency		Exergy Efficiency	
		Mean Square	F Value	Mean Square	F Value	Mean Square	F Value	Mean Square	F Value	Mean Square	F Value
IR power	2	165862.67	1090.40 **	712.03	356.18 **	1028.30	979.95 **	896.63	488.98 **	1483.96	296.30 **
T	2	203328.08	1336.70 **	827.16	413.77 **	1266.00	1206.47 **	1189.78	648.86 **	1848.15	369.01 **
RD	2	24350.56	160.08 **	77.98	39.01 **	122.19	116.44 **	159.96	87.24 **	212.27	42.38 **
IR * T	4	1129.06	7.42 **	28.49	14.25 **	24.48	23.33 **	40.834	22.26 **	16.85	3.36 *
IR * RD	4	277.10	1.82 ns	1.89	0.94 ns	0.75	0.71 ns	3.017	1.64 ns	1.81	0.36
T * RD	4	239.90	1.57 ns	0.79	0.39 ns	1.32	1.26 ns	5.943	3.24 ns	2.20	0.44
IR * T * RD	8	540.10	3.55 ns	2.458	1.22 ns	7.31	6.96 ns	7.004	3.82 ns	5.26	1.05
Error	54	152.111		1.999		1.049		1.834		5.008	

IR = infrared power; T = air temperature; RD = rotary rotation speed; \* = significant at 0.05; \*\* = significant at 0.01; ns = not significant; S.E.C = specific energy consumption.

### 3.2. Effective Moisture Diffusivity

Figure 4 shows the variance analysis related to the effect of the main parameters on the mean effective moisture diffusivity ( $D_{eff}$ ) during corn drying. The effect of the values of the main and interaction parameters on  $D_{eff}$  was significant at the 1% probability level. According to the results obtained (Figure 4), with the increase in all the main parameters,  $D_{eff}$  increases, which is described by the movement or mass transfer through the capillary pores of the food and the increase in water mobility. Therefore, these conditions lead to the acceleration of moisture removal from corn samples, the reduction in drying time and, consequently, the increase in  $D_{eff}$  [12]. The values of  $D_{eff}$  for corn drying ranged from  $4.75 \times 10^{-11}$  to  $6.62 \times 10^{-12}$  m<sup>2</sup>/s. Li et al. [7] and Abasi et al. [53] calculated the  $D_{eff}$  value for dried corn in the range of  $1.61 \times 10^{-11}$  to  $4.71 \times 10^{-11}$  m<sup>2</sup>/s and  $3.98 \times 10^{-11}$  to  $8.18 \times 10^{-11}$  m<sup>2</sup>/s, respectively. The highest  $D_{eff}$  value was obtained at a drying temperature of 65 °C, an

infrared power of 0.75 kW and a rotation speed of 12 rpm whereas the lowest  $D_{\text{eff}}$  value was recorded at a drying temperature of 45 °C, an infrared power of 0.25 kW and a rotation speed of 4 rpm.

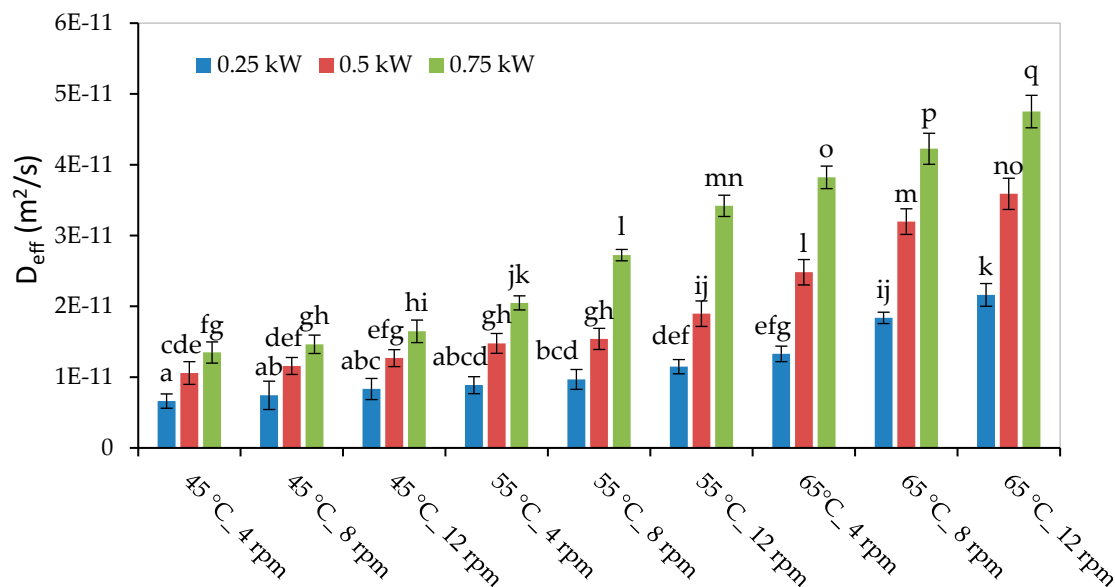


**Figure 4.** Effects of different drying conditions on  $D_{\text{eff}}$ . Different letters in the columns have a significant difference at the 1% probability level. Similar letters in each column indicate the absence of significant differences based on Duncan's test at the 5% probability level.

### 3.3. S.E.C, Energy and Thermal Efficiency

Table 2 shows the values of the S.E.C, energy and thermal efficiency of different conditions of drying corn in the CV-IR-D method. The results showed that the parameters of temperature, infrared power and rotary rotation speed in the CV-IR-D method affect the S.E.C, energy and thermal efficiency during the complete drying of corn (Table 1– $p < 0.01$ ). Therefore, S.E.C. decreased with rising drying temperature, IR power and rotary rotation speed while the energy and thermal efficiency increased under the mentioned conditions. This result was in agreement with the results reported by El-Mesery et al. [31], Singh et al. [27], Lemus-Mondaca et al. [40] and Motevali et al. [41]. They reported that decreasing drying time, IR power, temperature and rotary speed had significant effects on S.E.C., energy and thermal efficiency. The maximum S.E.C. and minimum energy and thermal efficiency were 28.15 MJ/kg, 3.24% and 5.5%, respectively, at a drying temperature of 45 °C, power of 0.25 kW and rotation speed of 4 rpm. According to the previous literature, increasing the drying time delays the evaporation of moisture from corn. Therefore, drying corn for a longer period of time results in a higher S.E.C. requirement [41,42]. On the other hand, the lowest S.E.C. and the highest values of energy efficiency and thermal efficiency were 5.06 MJ/kg, 29.31% and 32.31%, respectively, at a drying temperature of 65 °C, an infrared power of 0.75 kW and a rotation speed of 12 rpm. The S.E.C for drying corn using the fluidized bed method with ultrasonic pretreatment in the study of Abdoli et al. [8] was found to be in the range of 20.3 to 45.78 MJ/kg. In another study, the energy consumption for drying corn using the infrared method was determined to be in the range of 7.5 to 15 MJ/kg [10]. The S.E.C values reported in this study were lower than those observed in previous studies.

**Table 2.** Evaluation S.E.C, thermal efficiency and energy efficiency values of each drying condition.

Infrared Power (kW)	Drying Temperature (°C)	Rotary Rotation Speed (rpm)	S.E.C (MJ/kg)	Thermal Efficiency (%)	Energy Efficiency (%)
0.25	45	4	28.15 ± 1.95 <sup>o</sup>	5.50 ± 0.76 <sup>a</sup>	3.24 ± 0.98 <sup>a</sup>
0.25	45	8	25.96 ± 1.63 <sup>no</sup>	6.13 ± 0.91 <sup>a</sup>	4.66 ± 0.81 <sup>ab</sup>
0.25	45	12	24.67 ± 1.77 <sup>mn</sup>	7.04 ± 1.02 <sup>ab</sup>	6.01 ± 1.03 <sup>bc</sup>
0.25	55	4	22.56 ± 1.35 <sup>lm</sup>	7.79 ± 1.67 <sup>abc</sup>	6.89 ± 0.90 <sup>cd</sup>
0.25	55	8	21.68 ± 1.66 <sup>kl</sup>	9.14 ± 1.35 <sup>bcd</sup>	8.03 ± 0.71 <sup>de</sup>
0.25	55	12	19.47 ± 1.89 <sup>jk</sup>	10.28 ± 1.69 <sup>cde</sup>	8.99 ± 0.53 <sup>e</sup>
0.25	65	4	15.76 ± 1.74 <sup>i</sup>	10.23 ± 0.81 <sup>cde</sup>	12.42 ± 0.69 <sup>f</sup>
0.25	65	8	11.16 ± 1.03 <sup>fg</sup>	16.37 ± 0.92 <sup>h</sup>	17.80 ± 0.88 <sup>ij</sup>
0.25	65	12	9.55 ± 1.35 <sup>def</sup>	20.67 ± 1.53 <sup>ij</sup>	22.03 ± 0.53 <sup>k</sup>
0.5	45	4	21.38 ± 1.25 <sup>jkl</sup>	9.20 ± 0.97 <sup>bcd</sup>	8.11 ± 1.21 <sup>de</sup>
0.5	45	8	19.04 ± 1.63 <sup>j</sup>	10.56 ± 1.24 <sup>de</sup>	9.35 ± 0.71 <sup>e</sup>
0.5	45	12	16.50 ± 1.27 <sup>i</sup>	12.11 ± 0.71 <sup>ef</sup>	12.26 ± 1.46 <sup>f</sup>
0.5	55	4	14.06 ± 1.63 <sup>hi</sup>	13.14 ± 0.92 <sup>fg</sup>	14.01 ± 0.72 <sup>fg</sup>
0.5	55	8	12.50 ± 1.43 <sup>gh</sup>	14.98 ± 1.51 <sup>gh</sup>	16.06 ± 0.83 <sup>hi</sup>
0.5	55	12	11.07 ± 1.10 <sup>fg</sup>	16.97 ± 1.20 <sup>h</sup>	18.17 ± 0.92 <sup>j</sup>
0.5	65	4	9.24 ± 1.45 <sup>cdef</sup>	22.04 ± 1.46 <sup>jk</sup>	23.01 ± 1.02 <sup>kl</sup>
0.5	65	8	8.22 ± 0.60 <sup>bcde</sup>	24.26 ± 1.62 <sup>kl</sup>	24.78 ± 1.08 <sup>mn</sup>
0.5	65	12	7.09 ± 0.97 <sup>abcd</sup>	26.63 ± 1.20 <sup>m</sup>	26.50 ± 0.58 <sup>nop</sup>
0.75	45	4	15.77 ± 1.54 <sup>i</sup>	10.22 ± 1.01 <sup>cde</sup>	12.42 ± 1.32 <sup>f</sup>
0.75	45	8	14.76 ± 1.78 <sup>hi</sup>	12.97 ± 0.97 <sup>fg</sup>	14.54 ± 1.23 <sup>gh</sup>
0.75	45	12	12.35 ± 1.13 <sup>gh</sup>	16.22 ± 1.37 <sup>h</sup>	17.64 ± 1.31 <sup>ij</sup>
0.75	55	4	10.56 ± 1.54 <sup>efg</sup>	19.20 ± 1.32 <sup>i</sup>	21.28 ± 0.73 <sup>k</sup>
0.75	55	8	8.79 ± 0.99 <sup>cdef</sup>	23.00 ± 1.91 <sup>jk</sup>	24.04 ± 1.68 <sup>lm</sup>
0.75	55	12	7.86 ± 0.96 <sup>bcd</sup>	26.30 ± 1.97 <sup>lm</sup>	26.16 ± 1.39 <sup>no</sup>
0.75	65	4	6.71 ± 1.24 <sup>abc</sup>	27.41 ± 1.69 <sup>mn</sup>	27.37 ± 1.31 <sup>op</sup>
0.75	65	8	6.18 ± 1.20 <sup>ab</sup>	29.10 ± 1.69 <sup>no</sup>	28.10 ± 1.09 <sup>pq</sup>
0.75	65	12	5.06 ± 0.89 <sup>a</sup>	32.31 ± 1.74 <sup>o</sup>	29.31 ± 0.73 <sup>q</sup>

Different letters in the columns have a significant difference at the 1% probability level. Similar letters in each column indicate the absence of significant differences based on Duncan's test at the 5% probability level.

Increasing the rotary air speed results in a shorter drying process and a higher hot air circulation speed inside the chamber, leading to increased sample moisture evaporation, reduced time and energy consumption. In addition, it also increases energy and thermal efficiency. Such observations were found for the effect of rotary speed on drying and thermal efficiency by Kaveh et al. [42], who dried peas using a hot-air rotary dryer and reported energy and thermal efficiency in the range of 4.21–14.53% and 4.53–14.69%, respectively. Increasing infrared power and drying temperature leads to increased molecular mobility, moisture evaporation from the sample surface, drying rate and reduced drying time. Therefore, the thermal and energy efficiency values in the CV-IR-D dryer increased significantly ( $p < 0.05$ ).

### 3.4. Exergy Efficiency

Figure 5 shows the results obtained from the analysis of the average exergy efficiency of the corn drying process under different conditions of temperature, infrared power and rotary speed. As can be seen, the average exergy efficiency value was obtained from 22.21 to 55.35%. Which is comparable to the findings reported for drying dill leaves in an infrared drying system (55–66%) [48], potatoes in an infrared-hot air dryer (19.37–78.09%) [41] and for paddy in a convective dryer [54].

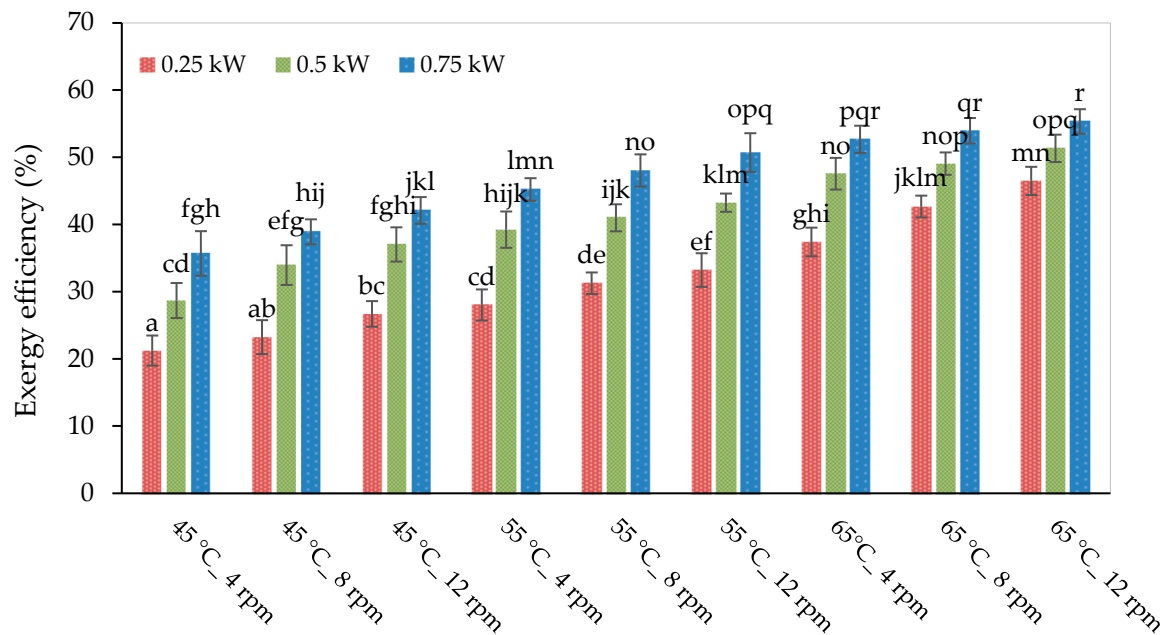


**Figure 5.** Exergy efficiency under different drying conditions. Different letters in the columns have a significant difference at the 1% probability level. Similar letters in each column indicate the absence of significant differences based on Duncan's test at the 5% probability level.

The results obtained show that the effect of infrared power, drying temperature and rotation speed leads to a significant increase ( $p < 0.01$ —Table 1) in the exergy efficiency. Similar results have been reported for drying apples [21], peas [19] and potatoes [43]. The increased rate of moisture removal from corn samples, the greater increase in exergy at the outlet of the drying chamber compared to the exergy entering the chamber and the significant reduction in the energy consumption of the drying system at high power, temperature and rotation speeds can be considered the main reasons for the increase in exergy efficiency [43,55].

### 3.5. Water Activity ( $W_a$ )

Since water is one of the most important factors in microbial, enzymatic and chemical spoilage in food, reducing and controlling  $W_a$  is a very effective method to increase shelf life and prevent adverse reactions (microbial growth and increased post-harvest losses) in food [56]. The results of the statistical analysis for  $W_a$  are shown in Table 3 and according to the table of main factors for  $W_a$ , it is statistically significant at the 1% level, but no significant interaction effect was obtained.

**Table 3.** ANOVA results of  $W_a$ , shrinkage, RR and  $\Delta E$  under different infrared power, air temperature and rotary rotation speed.

Parameter	df	Wa		Shrinkage		RR		$\Delta E$	
		Mean Square	F Value	Mean Square	F Value	Mean Square	F Value	Mean Square	F Value
IR power	2	0.03	81.62 **	71.55	101.99 **	1.24	73.43 **	133.34	113.67 **
T	2	0.03	96.64 **	604.30	861.40 **	6.76	398.57 **	598.94	510.60 **
RD	2	0.00	12.03 **	32.43	46.22 **	0.50	29.54 **	12.64	10.78 **
IR * T	4	0.00	0.73 ns	0.79	1.12 ns	0.04	2.44 ns	1.90	1.62
IR * RD	4	0.00	0.36 ns	0.24	0.34 ns	0.00	0.39 ns	0.07	0.06
T * RD	4	0.00	0.03 ns	0.44	0.63 ns	0.01	1.06 ns	0.70	0.60
IR * T * RD	8	0.00	0.62 ns	0.27	0.38 ns	0.00	0.18 ns	0.07	0.06

Error	54	0.00	0.70	0.01	1.17
-------	----	------	------	------	------

\* = significant at 0.05; \*\* = significant at 0.01; ns = not significant; Wa = water activity; RR = rehydration ratio; ΔE = color change.

Since most microbial, chemical and enzymatic reactions stop at Wa less than 0.6, it can be stated that corn prepared by the CV- IR-D drying method will have a long shelf life if stored properly and without moisture absorption, because the Wa of corn samples was in the range of 0.225–0.381 (Table 4). Therefore, dried corn samples can be considered microbially stable during storage.

**Table 4.** Color parameters and water activity of corn under different drying conditions.

Infrared Power (kW)	Drying Temperature (°C)	Rotary Rotation Speed (rpm)	L	a	b	ΔE	Wa
		Fresh	69.41 ± 1.62 <sup>k</sup>	5.77 ± 0.36 <sup>a</sup>	29.34 ± 0.92 <sup>n</sup>	-	0.905 ± 0.02 <sup>m</sup>
0.25	45	4	64.15 ± 2.19 <sup>j</sup>	5.99 ± 0.76 <sup>a</sup>	25.23 ± 0.97 <sup>m</sup>	16.22 ± 1.00 <sup>hijk</sup>	0.381 ± 0.01 <sup>l</sup>
0.25	45	8	63.16 ± 1.25 <sup>j</sup>	6.67 ± 0.30 <sup>ab</sup>	24.86 ± 0.96 <sup>lm</sup>	18.23 ± 0.66 <sup>kl</sup>	0.366 ± 0.01 <sup>kl</sup>
0.25	45	12	63.53 ± 2.22 <sup>j</sup>	6.24 ± 0.36 <sup>a</sup>	25.03 ± 0.83 <sup>lm</sup>	17.03 ± 0.97 <sup>ijk</sup>	0.359 ± 0.02 <sup>jkl</sup>
0.25	55	4	57.98 ± 1.81 <sup>cdef</sup>	9.00 ± 0.39 <sup>efg</sup>	18.10 ± 0.80 <sup>def</sup>	6.75 ± 1.02 <sup>a</sup>	0.352 ± 0.02 <sup>jkl</sup>
0.25	55	8	56.11 ± 1.25 <sup>abcdef</sup>	9.46 ± 0.55 <sup>ghi</sup>	17.27 ± 0.52 <sup>cde</sup>	7.78 ± 0.98 <sup>ab</sup>	0.343 ± 0.02 <sup>ijk</sup>
0.25	55	12	57.02 ± 1.65 <sup>bcdef</sup>	9.17 ± 0.41 <sup>fgh</sup>	17.99 ± 1.25 <sup>def</sup>	7.38 ± 1.04 <sup>a</sup>	0.331 ± 0.01 <sup>ijk</sup>
0.25	65	4	58.58 ± 2.00 <sup>defgh</sup>	7.59 ± 0.29 <sup>cd</sup>	22.19 ± 0.96 <sup>hijk</sup>	13.06 ± 0.65 <sup>de</sup>	0.326 ± 0.02 <sup>hij</sup>
0.25	65	8	57.98 ± 1.52 <sup>cdef</sup>	8.26 ± 0.45 <sup>def</sup>	21.57 ± 0.72 <sup>hi</sup>	13.98 ± 0.95 <sup>defg</sup>	0.286 ± 0.01 <sup>efg</sup>
0.25	65	12	58.37 ± 1.80 <sup>cdefg</sup>	7.89 ± 0.67 <sup>cd</sup>	21.87 ± 0.78 <sup>hi</sup>	13.47 ± 1.36 <sup>def</sup>	0.270 ± 0.02 <sup>bcdefg</sup>
0.5	45	4	59.60 ± 2.02 <sup>fghi</sup>	7.20 ± 0.67 <sup>bc</sup>	22.26 ± 0.87 <sup>hijk</sup>	20.28 ± 1.35 <sup>m</sup>	0.340 ± 0.02 <sup>ijk</sup>
0.5	45	8	58.62 ± 1.36 <sup>defgh</sup>	7.60 ± 0.54 <sup>cd</sup>	21.89 ± 1.14 <sup>hi</sup>	22.30 ± 0.77 <sup>n</sup>	0.331 ± 0.02 <sup>hij</sup>
0.5	45	12	59.03 ± 2.65 <sup>efghi</sup>	7.31 ± 0.32 <sup>bc</sup>	22.03 ± 0.89 <sup>hij</sup>	21.36 ± 1.36 <sup>mn</sup>	0.325 ± 0.02 <sup>hij</sup>
0.5	55	4	55.10 ± 1.99 <sup>abcd</sup>	10.90 ± 0.36 <sup>klm</sup>	15.70 ± 1.24 <sup>abc</sup>	12.19 ± 1.33 <sup>d</sup>	0.308 ± 0.02 <sup>ghi</sup>
0.5	55	8	53.12 ± 1.66 <sup>a</sup>	11.26 ± 0.40 <sup>m</sup>	14.93 ± 0.64 <sup>a</sup>	13.22 ± 1.65 <sup>de</sup>	0.291 ± 0.02 <sup>efgh</sup>
0.5	55	12	53.99 ± 1.25 <sup>ab</sup>	11.00 ± 0.42 <sup>lm</sup>	15.28 ± 1.13 <sup>ab</sup>	12.79 ± 0.58 <sup>de</sup>	0.283 ± 0.02 <sup>defg</sup>
0.5	65	4	56.65 ± 1.23 <sup>bcdef</sup>	10.00 ± 0.69 <sup>hijk</sup>	19.55 ± 1.08 <sup>fg</sup>	16.48 ± 0.77 <sup>hijk</sup>	0.262 ± 0.02 <sup>abcde</sup>
0.5	65	8	55.57 ± 1.83 <sup>abcde</sup>	10.46 ± 0.47 <sup>ijkl</sup>	18.78 ± 0.40 <sup>ef</sup>	17.85 ± 1.22 <sup>kl</sup>	0.255 ± 0.02 <sup>abcde</sup>
0.5	65	12	55.90 ± 1.23 <sup>abcde</sup>	10.24 ± 0.54 <sup>ijkl</sup>	19.06 ± 1.23 <sup>f</sup>	17.41 ± 0.95 <sup>jk</sup>	0.249 ± 0.02 <sup>abcd</sup>
0.75	45	4	62.12 ± 3.00 <sup>ij</sup>	7.99 ± 0.71 <sup>cd</sup>	23.85 ± 1.17 <sup>klm</sup>	18.18 ± 0.58 <sup>kl</sup>	0.324 ± 0.02 <sup>hij</sup>
0.75	45	8	61.59 ± 1.90 <sup>ghij</sup>	8.30 ± 0.34 <sup>def</sup>	23.37 ± 1.22 <sup>ijkl</sup>	20.14 ± 0.88 <sup>m</sup>	0.306 ± 0.01 <sup>fghi</sup>
0.75	45	12	61.89 ± 2.02 <sup>hij</sup>	8.12 ± 0.60 <sup>cde</sup>	23.69 ± 0.90 <sup>klm</sup>	19.68 ± 1.65 <sup>lm</sup>	0.288 ± 0.02 <sup>efg</sup>
0.75	55	4	56.54 ± 1.51 <sup>bcdef</sup>	9.57 ± 0.54 <sup>ghij</sup>	16.90 ± 0.99 <sup>bcd</sup>	9.27 ± 1.00 <sup>bc</sup>	0.280 ± 0.02 <sup>cdefg</sup>
0.75	55	8	54.87 ± 2.07 <sup>abc</sup>	10.26 ± 0.24 <sup>ijkl</sup>	15.97 ± 1.01 <sup>abc</sup>	10.03 ± 1.35 <sup>c</sup>	0.257 ± 0.01 <sup>abcde</sup>
0.75	55	12	55.11 ± 1.25 <sup>abcd</sup>	10.01 ± 0.64 <sup>hijk</sup>	16.35 ± 1.03 <sup>abcd</sup>	9.59 ± 1.25 <sup>bc</sup>	0.244 ± 0.01 <sup>abc</sup>
0.75	65	4	57.36 ± 1.22 <sup>bcdef</sup>	9.06 ± 0.68 <sup>fgh</sup>	21.66 ± 1.28 <sup>hi</sup>	14.58 ± 0.63 <sup>efgh</sup>	0.239 ± 0.01 <sup>ab</sup>
0.75	65	8	56.63 ± 1.98 <sup>bcdef</sup>	9.74 ± 0.43 <sup>ghij</sup>	20.75 ± 0.63 <sup>gh</sup>	15.75 ± 1.36 <sup>ghij</sup>	0.231 ± 0.01 <sup>a</sup>
0.75	65	12	56.93 ± 1.66 <sup>bcdef</sup>	9.47 ± 0.35 <sup>ghi</sup>	21.06 ± 0.83 <sup>gh</sup>	15.33 ± 0.70 <sup>fghi</sup>	0.226 ± 0.02 <sup>a</sup>

Different letters in the columns have a significant difference at the 1% probability level. Similar letters in each column indicate the absence of significant differences based on Duncan's test at the 5% probability level.

At a higher drying temperature, rotary rotation speed and infrared power, lower Wa (0.225) was observed (Table 4) because reducing the drying time caused a decrease in Wa. Due to the opening and structural change in the proteins, the ability of the samples to retain bound water decreases and water evaporates more quickly from the surface of the corn samples, which in turn affects the reduction in the Wa of the samples [57]. On the other hand, the highest Wa (0.381) was determined in the sample with a drying temperature of 45 °C, a rotation speed of 4 rpm and an infrared power of 0.25 kW. An et al. [15] and Antal et al. [58] in their research on corn using different drying methods reported the Wa values in the range of 0.41–0.47 and 0.211–0.361, respectively.

### 3.6. Color

In this study, the average initial values of brightness, redness and yellowness indices for fresh corn samples were 69.41, 5.57 and 29.34, respectively. The results of the statistical analysis for color changes are shown in Table 5. According to this table, the factors of infrared power, drying temperature and rotary rotation speed on color parameters are statistically significant at the 5% level. According to Table 4, it can be seen that the color characteristics ( $L^*a^*b^*$ ) produce darker compounds as the drying process progresses due to the presence of heat-sensitive (thermosensitive) material in corn, and as a result, corn samples tend to decrease in brightness. According to the results shown in Table 4, the value of  $L^*$  (an index for determining the brightness or darkness of the color of the samples) gradually decreases and then increases slightly with rising IR power, drying temperature and rotary rotation speed. Therefore, the lowest  $L^*$  value was obtained at 0.5 kW infrared power, 55 °C drying temperature and 8 rpm rotation speed. Jibril et al. [12] suggested that the darkening and reduction in corn color quality is due to carotenoid degradation reactions and Maillard reaction.

**Table 5.** ANOVA results of  $L^*$ ,  $a^*$  and  $b^*$  under different infrared power, air temperature and rotary rotation speed.

Parameter	df	$L^*$		$a^*$		$b^*$	
		Mean Square	F Value	Mean Square	F Value	Mean Square	F Value
IR power	2	71.59	21.67 **	24.92	94.97 **	50.88	53.76 **
T	2	259.93	78.70 **	58.76	223.97 **	342.66	362.02 **
RD	2	9.21	2.78 <sup>ns</sup>	1.52	5.82 **	3.03	3.20 *
IR * T	4	3.45	1.04 <sup>ns</sup>	2.59	9.87 **	0.63	0.66 <sup>ns</sup>
IR * RD	4	0.10	0.03 <sup>ns</sup>	0.02	0.09 <sup>ns</sup>	0.03	0.04 <sup>ns</sup>
T * RD	4	0.82	0.25 <sup>ns</sup>	0.04	0.18 <sup>ns</sup>	0.13	0.14 <sup>ns</sup>
IR * T * RD	8	0.06	0.02 <sup>ns</sup>	0.01	0.04 <sup>ns</sup>	0.01	0.02 <sup>ns</sup>
Error	54	3.30		0.26		0.94	

\* = significant at 0.05; \*\* = significant at 0.01; ns = not significant.

Increasing temperature, IR power and rotary rotation speed first increased the value of  $a^*$  (an index to determine the amount of redness of the samples) from 5.99 to 11.26 (darkening of the red color) and then slightly decreased it to 7.60. However, the highest value of  $a^*$  was determined at an infrared power, drying temperature and rotary rotation speed of 0.5 kW, 55 °C and 8 rpm, respectively. According to the study of Jibril et al. [12], the most important factors for sensitivity to redness at infrared power, drying temperature and medium rotary rotation speed can be carotenoid pigments and chlorophyll present in corn grains.

In this study, the  $b^*$  obtained varied between 14.93 and 25.23 and was comparable to the result obtained by Abdoli et al. [8], who obtained  $b^*$  values for corn ranging from about 9 to 31. The lower  $b^*$  values in the medium treatments may be due to thermal degradation of pigments. Table 3 shows the effect of the main parameters on the color change index ( $\Delta E$ ) of dried corn. A significant difference was observed between infrared powers, drying temperature and rotary rotation speed ( $p < 0.01$ ). Increasing the infrared power from 0.25 to 0.5 kW and the drying temperature from 45 to 55 °C at different rotary speeds had a decreasing effect on the color change process, indicating an improvement in color and the prevention of color change (reduction in product marketability). Increasing the infrared power to 0.75 kW and the drying temperature to 65 °C increased the color change ( $p < 0.05$ ).

### 3.7. Rehydration Ratio

The rehydration coefficient is one of the important properties used to measure the quality of dried food and can also be considered as a measure of damage caused by drying. Slow or poor RR is due to internal tissue collapse [34]. According to the data obtained and statistical studies, the RR rate among the different treatments of this study, including the effect of infrared power, temperature and rotation speed on dried corn, is shown in Table 6. Table 3 showed that there was a significant difference in terms of RR between all the main treatments ( $p < 0.01$ ). The average RR of all the samples was in the range of 1.87 to 3.55. In the study of Jibril et al. [12] and Antal et al. [58], the RR for corn was reported to be 2.22 to 3.08 and 2.04 to 3.48, respectively. Also, a significant effect of infrared power and air temperature on garlic rehydration has been reported [29]. With increasing temperature and infrared power at a constant rotary speed, the RR initially increased by 71%, then it decreased by 30%. Therefore, the lowest RR value was associated with a drying temperature of 45 °C, a rotation speed of 4 rpm, and an infrared power of 0.25 kW. This can be explained by the damage to the cell structure (collapsed cells) and also the lower water diffusion in corn samples at lower temperatures and infrared powers [59]. In addition, the highest RR was achieved at a temperature of 55 °C, an infrared power of 0.5 kW and a rotary speed of 4 rpm. At medium temperatures, infrared power and rotary speed, the matrix structure in corn samples was better preserved. On the other hand, RR was improved at high infrared temperatures and powers (70 °C and 0.75 kW) compared to low temperatures and powers (45 °C and 0.25 kW) due to the effect of heat on the cell wall and tissue [39].

**Table 6.** Rehydration ratio and shrinkage of corn under different drying conditions.

Infrared Power (kW)	Drying Temperature (°C)	Rotary Rotation Speed (rpm)	Shrinkage (%)	RR
0.25	45	4	18.56 ± 1.22 <sup>o</sup>	1.87 ± 0.12 <sup>a</sup>
0.25	45	8	16.99 ± 0.81 <sup>n</sup>	2.05 ± 0.22 <sup>abc</sup>
0.25	45	12	17.63 ± 0.73 <sup>no</sup>	1.94 ± 0.11 <sup>ab</sup>
0.25	55	4	9.69 ± 0.68 <sup>efg</sup>	2.69 ± 0.12 <sup>ij</sup>
0.25	55	8	6.59 ± 0.45 <sup>bc</sup>	2.95 ± 0.15 <sup>kl</sup>
0.25	55	12	8.45 ± 0.93 <sup>de</sup>	2.81 ± 0.13 <sup>jk</sup>
0.25	65	4	14.26 ± 1.41 <sup>kl</sup>	2.24 ± 0.14 <sup>cdef</sup>
0.25	65	8	12.57 ± 0.75 <sup>ij</sup>	2.44 ± 0.18 <sup>fgh</sup>
0.25	65	12	13.55 ± 1.02 <sup>jk</sup>	2.32 ± 0.06 <sup>defg</sup>
0.5	45	4	15.43 ± 0.79 <sup>lm</sup>	2.08 ± 0.09 <sup>abc</sup>
0.5	45	8	13.69 ± 1.21 <sup>jk</sup>	2.38 ± 0.18 <sup>efg</sup>
0.5	45	12	15.03 ± 1.04 <sup>klm</sup>	2.22 ± 0.11 <sup>cdef</sup>
0.5	55	4	6.63 ± 0.42 <sup>bc</sup>	3.14 ± 0.13 <sup>lm</sup>
0.5	55	8	4.51 ± 0.67 <sup>a</sup>	3.55 ± 0.12 <sup>o</sup>
0.5	55	12	5.12 ± 0.99 <sup>ab</sup>	3.29 ± 0.15 <sup>mn</sup>
0.5	65	4	10.45 ± 0.60 <sup>gh</sup>	2.72 ± 0.16 <sup>ijk</sup>
0.5	65	8	8.59 ± 0.69 <sup>def</sup>	2.96 ± 0.08 <sup>kl</sup>
0.5	65	12	9.63 ± 0.57 <sup>efg</sup>	2.81 ± 0.13 <sup>jk</sup>
0.75	45	4	17.11 ± 0.68 <sup>no</sup>	2.01 ± 0.13 <sup>abc</sup>
0.75	45	8	14.77 ± 0.38 <sup>kl</sup>	2.18 ± 0.10 <sup>bcde</sup>
0.75	45	12	16.30 ± 0.97 <sup>mn</sup>	2.12 ± 0.09 <sup>bcd</sup>
0.75	55	4	7.89 ± 0.89 <sup>cd</sup>	2.94 ± 0.06 <sup>kl</sup>
0.75	55	8	5.25 ± 0.78 <sup>ab</sup>	3.38 ± 0.09 <sup>no</sup>
0.75	55	12	6.23 ± 0.79 <sup>b</sup>	3.11 ± 0.11 <sup>lm</sup>
0.75	65	4	12.66 ± 0.70 <sup>ij</sup>	2.51 ± 0.13 <sup>ghi</sup>

0.75	65	8	10.01 ± 0.91 <sup> fgh</sup>	2.73 ± 0.08 <sup> ijk</sup>
0.75	65	12	11.33 ± 0.45 <sup> hi</sup>	2.62 ± 0.17 <sup> hij</sup>

Different letters in the columns have a significant difference at the 1% probability level. Similar letters in each column indicate the absence of significant differences based on Duncan's test at the 5% probability level.

### 3.8. Shrinkage

The effect of the main drying parameters on the shrinkage rate of corn was significant at the 1% probability level (Table 3). However, considering that the lowest amount of shrinkage is expected, the treatment of 0.5 kW, 55 °C and 8 rpm was the best method for drying corn in terms of shrinkage (Table 6) because under the aforementioned conditions it had a higher water delivery capacity and a faster water absorption rate. The shrinkage rate for the corn samples was in the range of 4.5 to 18.55%, which is somewhat consistent with the study of Abdoli et al. [8] (i.e., 3 to 13.13%). Low temperature, infrared power and rotary rotation speed, due to the hardening of the shell and the reduction in the effective surface area, cause stress in the cell structure and ultimately change in the dimensions, shape or volume of the material (shrinkage); then, by damaging the capillary tubes it causes a decrease in water absorption, resulting in an increase in the shrinkage rate [60]. El-Mesery et al. [57] observed more shrinkage at lower infrared power. Ghasemkhani et al. [26] showed that the lowest drying temperature had the highest shrinkage and the medium rotary speed had the lowest shrinkage.

### 3.9. ANNs

ANN modeling was used to predict the drying time, S.E.C, energy efficiency, thermal efficiency and exergy of dried corn in the CV-IR-D system. Laboratory data obtained from the drying process were used to train and evaluate the network. The results obtained from using artificial neural networks to predict the desired parameters are reported in Table 7. The process started with a low number of neurons (two neurons) in the hidden layer and the addition of neurons continued until the addition of more neurons had no effect on improving the error; for this purpose, 2 to 20 neurons were used in the hidden layer. A network with 15 neurons in the first hidden layer was the best network in the drying time modeling process (i.e., topology 3-15-1). Topologies 3-14-15-1, 3-16-1, 3-13-1 and 3-20-1 were selected as the best topologies for predicting S.E.C, energy efficiency, thermal efficiency and exergy efficiency, respectively. The high values of R reported in Table 7 indicate the high efficiency of the ANN. According to Figure 6, the R values of the training data for predicting drying time (a), S.E.C. (b), energy efficiency (c), thermal efficiency (d) and exergy efficiency (e) were obtained as 0.9938, 0.9906, 0.9965, 0.9874 and 0.9893, respectively, while the mean square error values were determined as 0.000314, 0.000836, 0.000564, 0.000798 and 0.000857. As can be seen in Figure 6, the values of the R<sup>2</sup> for the training, validation, test and all data have desirable values, and the closer it is to one, the more successful the prediction process. For example, the R is higher than 0.98 for all data, which indicates a successful prediction by artificial neural networks.

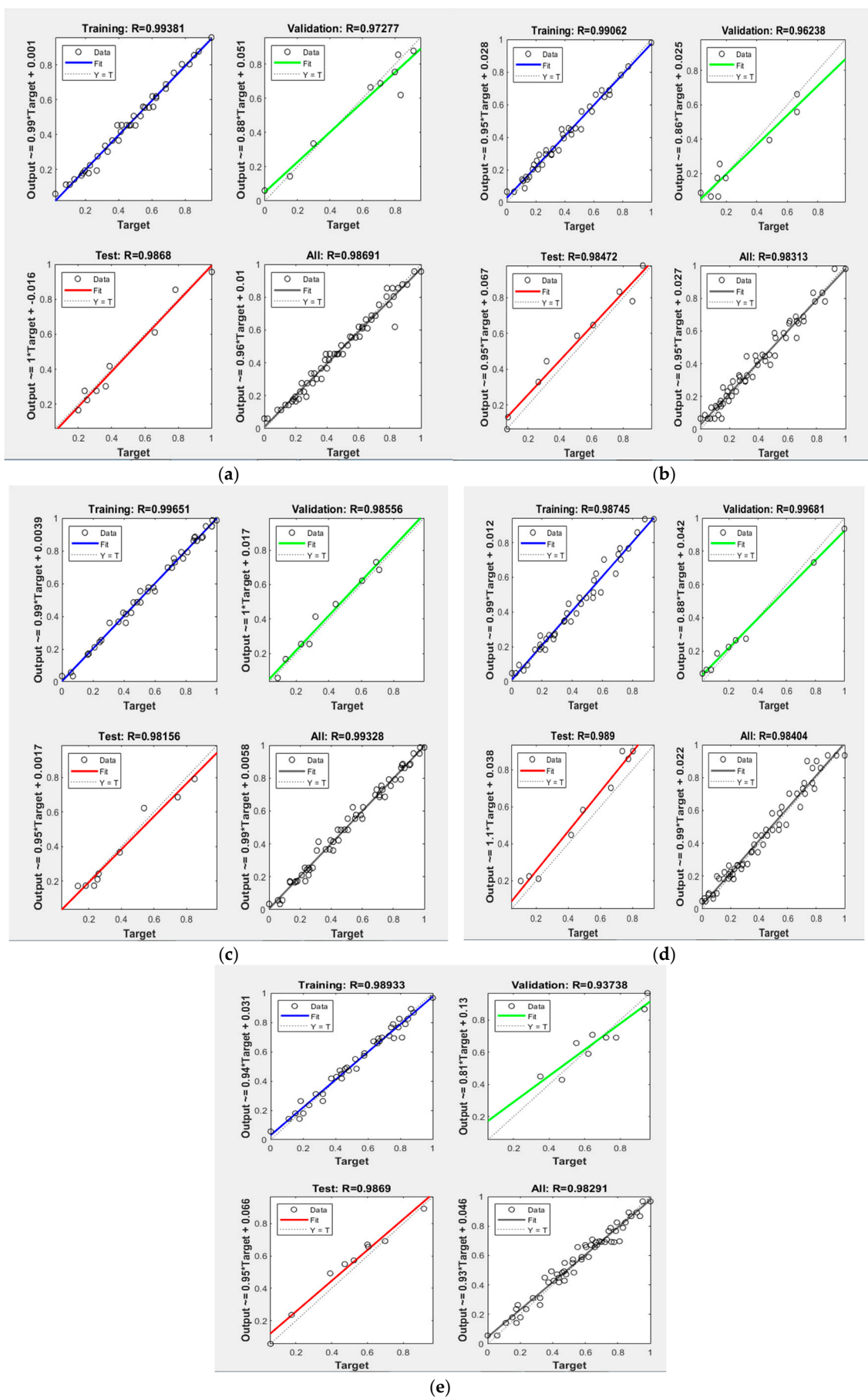


**Figure 6.** Regressions of the ANN modeling of CV-IR-D dried corn: (a) drying time, (b) S.E.C, (c) energy efficiency, (d) thermal efficiency and (e): exergy efficiency.

**Table 7.** Statistical results of drying time, S.E.C, thermal, energy and exergy efficiency with ANN model.

Parameter	Number of Hidden Layer (s)	Threshold Function	Topology	MSE	R (Training)	R (Testing)	Training Epoch
Time	1	Tan-Tan	3-15-1	0.00031	0.9938	0.9868	11
	1	Log-Tan	3-10-1	0.00036	0.9910	0.9586	9
	1	Log-Tan	3-18-1	0.00039	0.9856	0.9505	9
	1	Tan-Pur	3-13-1	0.00032	0.9877	0.9836	8
	2	Tan-Log-Tan	3-15-13-1	0.00037	0.9895	0.9752	23
	2	Tan-Pur-Tan	3-18-16-1	0.00032	0.9935	0.9756	12
	2	Log-Tan-Tan	3-12-12-1	0.00043	0.9849	0.9408	10
	2	Log-Tan-Pur	3-9-9-1	0.00042	0.9891	0.9488	7
S.E.C	1	Tan-Tan	3-13-1	0.00090	0.9845	0.9468	8
	1	Log-Tan	3-16-1	0.00093	0.9836	0.9521	9
	1	Log-Pur	3-8-1	0.00096	0.9901	0.9447	11
	1	Tan-Tan	3-20-1	0.00098	0.9795	0.9865	15
	2	Tan-Tan-Pur	3-10-10-1	0.00086	0.9846	0.9766	7
	2	Tan-Log-Pur	3-7-6-1	0.00089	0.9715	0.9792	13
	2	Pur-Tan-Tan	3-15-14-1	0.00083	0.9906	0.9847	10
	2	Tan-Tan-Tan	3-9-9-1	0.00094	0.9456	0.9854	10
Energy efficiency	1	Tan-Tan	3-8-1	0.00059	0.9890	0.9801	11
	1	Log-Tan	3-12-1	0.00057	0.9957	0.9798	8
	1	Log-Pur	3-16-1	0.00056	0.9965	0.9815	6
	1	Tan-Pur	3-15-1	0.00064	0.9840	0.9488	7
	2	Tan-Tan-Tan	3-15-10-1	0.00057	0.9963	0.9808	11
	2	Tan-Tan-Log	3-6-5-1	0.00062	0.9868	0.9624	17
	2	Log-Tan-Tan	3-10-10-1	0.00060	0.9905	0.9756	15
	2	Tan-Log-Tan	3-20-20-1	0.00063	0.9891	0.9763	9
Thermal efficiency	1	Tan-Tan	3-13-1	0.00079	0.9874	0.9890	17
	1	Log-Tan	3-11-1	0.00082	0.9859	0.9860	8
	1	Tan-Tan	3-17-1	0.00089	0.9721	0.9678	9
	1	Tan-Log	3-8-1	0.00090	0.9702	0.9756	13
	2	Tan-Log-Tan	3-18-15-1	0.00081	0.9864	0.9840	8
	2	Log-Tan-Pur	3-10-9-1	0.00080	0.9858	0.9510	8
	2	Log-Tan-Tan	3-15-15-1	0.00084	0.9848	0.9838	10
	2	Tan-Tan-Tan	3-12-12-1	0.00091	0.9611	0.9723	14
Exergy efficiency	1	Tan-Tan	3-20-1	0.00085	0.9893	0.9869	11
	1	Log-Tan	3-11-1	0.00086	0.9866	0.9852	8
	1	Log-Pur	3-7-1	0.00089	0.9653	0.9811	13
	1	Tan-Tan	3-14-1	0.00092	0.9711	0.9536	9
	2	Tan-Log-Tan	3-18-14-1	0.00086	0.9832	0.9799	8
	2	Log-Tan-Pur	3-20-18-1	0.00092	0.9563	0.9611	5
	2	Tan-Tan-Pur	3-8-8-1	0.00091	0.9696	0.9468	11
	2	Tan-Tan-Tan	3-6-5-1	0.00088	0.9769	0.9699	13

Figure 7 shows the obtained mean square error values. It can be clearly seen in Figure 7 that the best error results are obtained for the training, validation and test data in epochs 6 (drying time), 4 (S.E.C), 4 (energy efficiency), 11 (thermal efficiency) and 5 (exergy efficiency). In fact, the downward trend of the error is very desirable, and the closer we get to zero, the more desirable the result. The exact values of the mean square error are shown in Table 7.

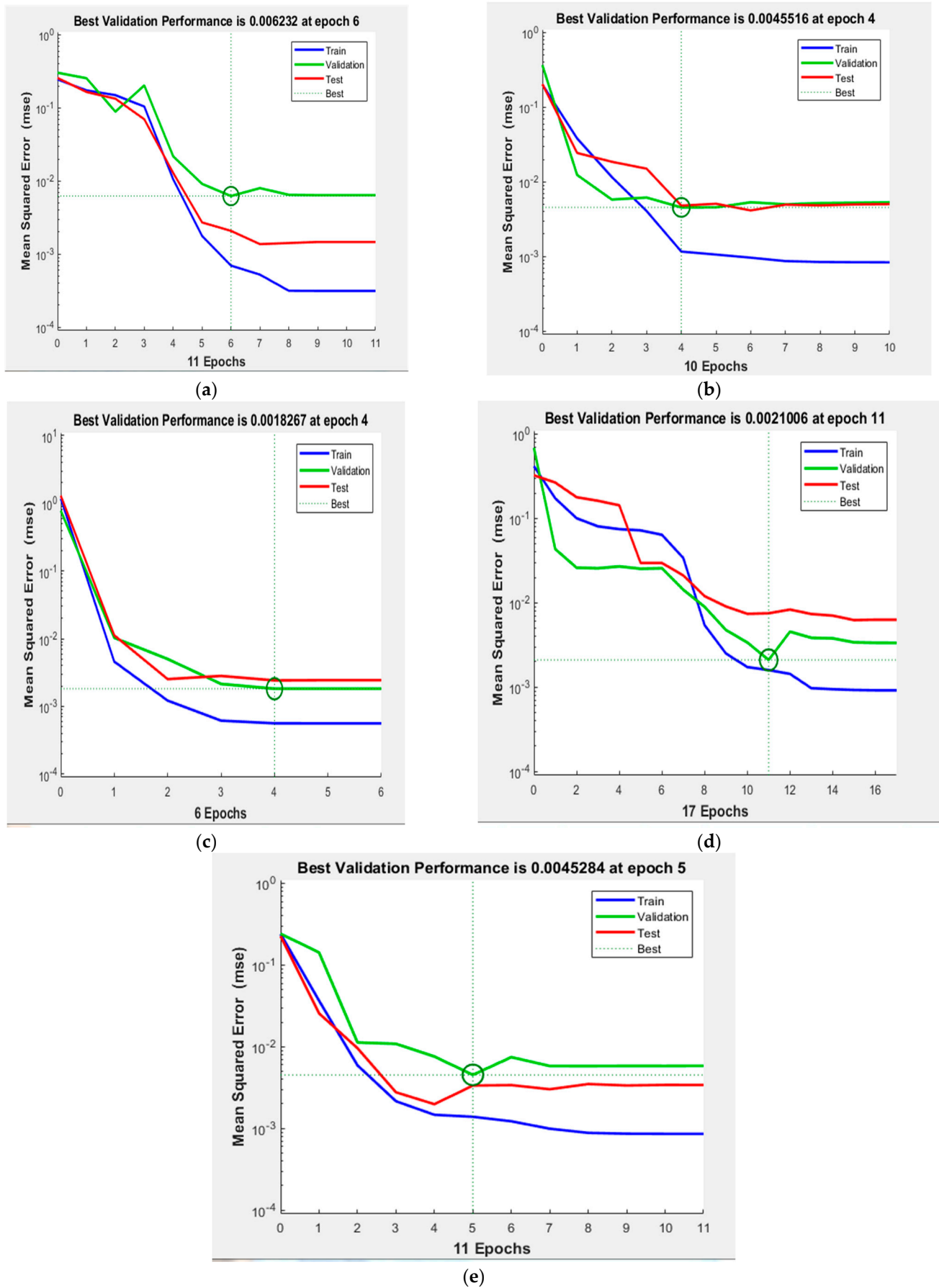


Figure 7. Best validation performance of the ANN modeling of CV-IR-D dried corn: (a) drying time, (b) S.E.C, (c) energy efficiency, (d) thermal efficiency and (e) exergy efficiency.

Liu et al. [61] used an artificial neural network to model and predict energy and exergy parameters of mushroom during hot air drying. For this purpose, a multilayer perceptron artificial neural network was used under the name of forward backpropagation. Their results showed that the used neural network has great potential to provide acceptable results of energy parameters in the drying system. Other studies have reported the use of artificial neural networks in predicting drying parameters [62–66].

There is no reliable theory governing the best way to choose an appropriate network structure for a given problem in drying technology. Therefore, choosing an ANN structure for a typical application in drying technology is problematic, because most of the developed ANN models are usually determined by experience or trial and error. In addition, standard ANN models are still subject to overtraining, adaptation and validation problems. On the other hand, ANNs do not allow for the interpretation of model parameters and do not provide much insight into the relative importance of different input variables. Therefore, these inherent limitations of artificial neural networks may jeopardize their use in real drying technology [67].

### *3.10. The Limitations of the Research and Future Perspectives*

The development, or construction, of a laboratory dryer is still a complex and highly constrained task that requires the consideration of multiple aspects. On the other hand, the design of a hybrid dryer requires multiple considerations that require consideration of economic feasibility (affordability), environmental sustainability (environmentally friendly) and optimization of energy consumption and/or product quality. With the recent advances in AI technologies in the food industry, the current landscape of the food drying industry has changed and offers a promising future in terms of food quality, energy reduction and public acceptance of food. Rapid advances in digital and software technology have facilitated the integration of AI into drying technologies.

## **4. Conclusions**

In the present study, corn samples were dried under different conditions (temperature, infrared power and rotation speed) using the CV-IR-D method and quality, S.E.C, energy, thermal and exergy efficiency indices were studied. The mentioned variables were effective on the drying time, energy parameters and exergy efficiency of corn samples. According to thermodynamic analyses, it was found that with the increasing temperature, infrared power and rotary rotation speed in the drying chamber, the S.E.C decreased, while energy efficiency, thermal efficiency and exergy efficiency increased. The minimum and maximum S.E.C, energy efficiency, thermal efficiency and exergy efficiency were equal to 5.06–28.15 MJ/kg, 3.24–29.31, 5.50–32.31% and 21.24–55.34%, respectively. On the other hand, with increasing infrared power, drying temperature and rotary rotation speed, the amount of moisture removed from the samples and the moisture diffusion coefficient increased and the drying time decreased. Due to the porous structure of the corn samples at a higher power, temperature and rotation speed, the mass and heat transfer rate during the drying process increased. Also, the possibility of drying food at infrared temperature and power and medium rotary rotation speed (55 °C and 0.5 kW and 8 rpm) causes the dried sample to absorb water faster (higher RR) and reduce product shrinkage. In addition, color changes were also minimal under these conditions. Artificial neural network modeling was used to predict drying time, specific energy consumption, energy, thermal and exergy efficiency as a function of infrared power, rotary rotation speed and drying temperature during drying by the CV-IR-D method. Based on the data analysis, the networks with the structure 3-15-1, 3-14-15-1, 3-16-1, 3-13-1 and 3-20-1 were the most suitable networks for estimating drying time, S.E.C, energy efficiency, thermal efficiency and exergy efficiency of corn, respectively.

**Author Contributions:** Y.A.-G.: investigation, supervision, conceptualization, data curation, data analysis and writing—original draft preparation. M.K.: conceptualization, methodology, validation, software, writing—review and editing and investigation. S.Z.: data curation, data analysis and writing—original draft preparation. S.H.: methodology, validation, writing—review and editing and investigation. M.S.: formal analysis, resources, project administration. K.W.: writing—review and editing. All authors have read and agreed to the published version of the manuscript.

**Funding:** This research received no external funding

**Data Availability Statement:** All data and materials are available upon reasonable request from the corresponding author.

**Conflicts of Interest:** The authors declare no conflicts of interest.

## Abbreviations

A	m <sup>2</sup>	Area of tray in which sample is placed
C <sub>a</sub>	J/kg °C	Specific heat
D <sub>eff</sub>	m <sup>2</sup> /s	Effective moisture diffusivity
D <sub>t</sub>	h	Total drying time of each sample
D <sub>w</sub>	Kg/m <sup>2</sup>	Weight density of foamed sample
$EX_{dest}$	kJ	Exergy destruction in the system
$EX_{in}$	kJ	Total exergy inflow
$EX_{out}$	kJ	Total exergy outflow
EU <sub>ter</sub>	kJ	Thermal energy consumption in convective dryer
EU <sub>mec</sub>	kJ	Mechanical energy consumption
EU <sub>IR</sub>	kJ	Thermal energy consumption in infrared dryer
EU <sub>D</sub>	kJ	Thermal energy consumption in rotary dryer
h <sub>ig</sub>	J/kg	Latent heat of evaporation of sample
M <sub>e</sub>	% d.b	Equilibrium moisture contents
MR	-	Moisture ratio
M <sub>w</sub>	kg	Weight of moisture evaporated from the sample
M <sub>o</sub>	% d.b	Final moisture content of the sample
M <sub>t</sub>	% d.b	Moisture content at time t
M <sub>i</sub>	% d.b	Initial moisture content of the corn sample
N	-	Number of training data
K	W	Infrared power
O <sub>i</sub>	-	Value predicted by the ANN for the i <sup>th</sup> pattern
Q	-	Represents the moisture removed per unit time
Q <sub>w</sub>	(kJ)	Consumed energy for the moisture evaporation
R	8.314 J/mol. K	Universal gas constant
R <sup>2</sup>		Correlation coefficient
r <sub>e</sub>	m	Equivalent radius of corn
S <sub>gen</sub>	kJ/K	Has produced entropy after the process
SEC	MJ/kg	Specific energy consumption
t	s	Drying time
TE	%	Thermal efficiency
T <sub>0</sub>	K	Dead-state temperature
T <sub>i</sub>	-	Target (trial) value for the i <sup>th</sup> pattern
T <sub>m</sub>	-	Average of predicted values
v	m/s	Drying air velocity
W <sub>r</sub>	kg	Initial mass of product
W <sub>d</sub>	kg	Mass of dried product (kg)
X <sub>wf</sub>	%d.b	Final moisture content of dried samples
Y	W	The power of electrical motors used in different parts of dryer
X <sub>i</sub>		stands for each parameter
X <sub>max</sub>		Maximum data for each parameter

$X_{\min}$		Minimum data for each parameter
$Q_a$	Kg/m <sup>3</sup>	Density of air
$\eta_{ex}$	%	Exergy efficiency
$\eta_e$	%	Energy efficiency
$\Delta L^*, \Delta b^*, \Delta a^*$	-	The difference between the color of fresh and dried samples
$\Delta T$	°C	Drying temperature
$\Delta P$	mbar	Different pressure

## References

- Cui, J.; Ren, H.; Wang, B.; Chang, F.; Zhang, X.; Meng, H.; Jiang, S.; Tang, J. Hatching and development of maize cyst nematode *Heterodera zae* infecting different plant hosts. *J. Integr. Agric.* **2024**, *23*, 1593–1603.
- Zhang, M.; Hu, Y.; Han, W.; Chen, J.; Lai, J.; Wang, Y. Potassium nutrition of maize: Uptake, transport, utilization, and role in stress tolerance. *Crop J.* **2023**, *11*, 1048–1058.
- Hasnaki, R.; Ziaee, M.; Mahdavi, V. Pesticide residues in corn and soil of corn fields of Khuzestan, Iran, and potential health risk assessment. *J. Food Compos. Anal.* **2023**, *115*, 104972.
- Wei, S.; Tian, B.; Fan, H.; Ren, G.; Yang, D.; Ai, Z. Radiofrequency assisted hot air drying of corn kernels: Drying characteristics, uniformity, quality, and energy consumption. *Drying Technol.* **2024**, *42*, 1846–1854.
- Mondal, M.H.T.; Akhtaruzzaman, M.; Sarker, M.S.H. Modeling of dehydration and color degradation kinetics of maize grain for mixed flow dryer. *J. Agric. Food Res.* **2022**, *9*, 100359.
- Kumar, A.; Kandasamy, P.; Chakraborty, I.; Hangshing, L. Analysis of energy consumption, heat and mass transfer, drying kinetics and effective moisture diffusivity during foam-mat drying of mango in a convective hot-air dryer. *Biosyst. Eng.* **2022**, *219*, 85–102.
- Li, S.; Chen, S.; Liang, Q.; Ma, Z.; Han, F.; Xu, Y.; Jin, Y.; Wu, W. Low temperature plasma pretreatment enhances hot-air drying kinetics of corn kernels. *J. Food Process Eng.* **2019**, *42*, e13195.
- Abdoli, B.; Zare, D.; Jafari, A.; Chen, G. Evaluation of the air-borne ultrasound on fluidized bed drying of shelled corn: Effectiveness, grain quality, and energy consumption. *Drying Technol.* **2018**, *36*, 1749–1766.
- Vukić, M.; Janevski, J.; Vučković, G.; Stojanović, B.; Petrović, A. Experimental investigation of the drying kinetics of corn in a packed and fluidized bed. *Iran. J. Chem. Chem. Eng.* **2015**, *34*, 43–49.
- Wilson, S.A.; Okeyo, A.A.; Olatunde, G.A.; Atungulu, G.G. Radiant heat treatments for corn drying and decontamination. *J. Food Process. Preserv.* **2017**, *41*, e13193.
- Rahmanian-Koushkaki, H.; Nourmohamadi-Moghadami, A.; Zare, D.; Karimi, G. Experimental and theoretical investigation of hot air-infrared thin layer drying of corn in a fixed and vibratory bed dryer. *Eng. Agric. Environ. Food* **2017**, *10*, 191–197.
- Jibril, A.N.; Zuo, Y.; Wang, S.; Kibiya, A.Y.; Attanda, M.L.; Henry, I.I.; Huang, J.; Chen, K. Influence of drying chamber, energy consumption, and quality characterization of corn with graphene far infrared dryer. *Drying Technol.* **2024**, *42*, 1875–1890.
- De Faria, R.Q.; Dos Santos, A.R.P.; Garipey, Y.; Da Silva, E.A.A.; Sartori, M.M.P.; Raghavan, V. Optimization of the process of drying of corn seeds with the use of microwaves. *Drying Technol.* **2020**, *38*, 676–684.
- Liu, H.; Liu, H.; Liu, H.; Zhang, X.; Hong, Q.; Chen, W.; Zeng, X. Microwave drying characteristics and drying quality analysis of corn in China. *Processes* **2021**, *9*, 1511.
- An, N.N.; Sun, W.; Li, D.; Wang, L.J.; Wang, Y. Effect of microwave-assisted hot air drying on drying kinetics, water migration, dielectric properties, and microstructure of corn. *Food Chem.* **2024**, *455*, 139913.
- Al-Hilphy, A.R.; Al-Mtury, A.A.A.; Al-Iessa, S.A.; Gavahian, M.; Al-Shatty, S.M.; Jassim, M.A.; Mohusen, Z.A.A.; Khaneghah, A.M. A pilot-scale rotary infrared dryer of shrimp (*Metapenaeus affinis*): Mathematical modeling and effect on physicochemical attributes. *J. Food Process Eng.* **2022**, *45*, e13945.
- Yamchi, A.A.; Sharifian, F.; Khalife, E.; Kaveh, M. Drying kinetic, thermodynamic and quality analyses of infrared drying of truffle slices. *J. Food Sci.* **2024**, *89*, 3666–3686.
- Alshehri, A.A.; Tolba, N.M.; Salama, M.A.; Saleh, M.; Kamel, R.M. Energy analysis and quality characteristics of flaxseed oil by using an infrared rotary dryer. *Case Stud. Therm. Eng.* **2024**, *54*, 103988.
- Kaveh, M.; Abbaspour-Gilandeh, Y.; Chen, G. Drying kinetic, quality, energy and exergy performance of hot air-rotary drum drying of green peas using adaptive neuro-fuzzy inference system. *Food Bioprod. Process.* **2020**, *124*, 168–183.
- Balakrishnan, M.; Jeevarathinam, G.; Aiswariya, S.; Ambrose, R.K.; Ganapathy, S.; Pandiselvam, R. Design, development, and evaluation of rotary drum dryer for turmeric rhizomes (*Curcuma longa* L.). *J. Food Process Eng.* **2022**, *45*, e14052.

21. Ghasemkhani, H.; Keyhani, A.; Aghbashlo, M.; Rafiee, S.; Mujumdar, A.S. Improving exergetic performance parameters of a rotating-tray air dryer via a simple heat exchanger. *Appl. Therm. Eng.* **2016**, *94*, 13–23.
22. Bassey, E.J.; Cheng, J.H.; Sun, D.W. Improving drying kinetics, physicochemical properties and bioactive compounds of red dragon fruit (*Hylocereus* species) by novel infrared drying. *Food Chem.* **2022**, *375*, 131886.
23. Kaveh, M.; Abbaspour-Gilandeh, Y.; Nowacka, M.; Kalantari, D.; El-Mesery, H.S.; Taghinezhad, E. Energy and exergy analysis of drying terebinth in a far infrared-rotary dryer using response surface methodology. *Heat Transf.* **2024**, *53*, 4109–4134.
24. Pradechboon, T.; Dussadee, N.; Unpaprom, Y.; Chindaraksa, S. Effect of rotary microwave drying on quality characteristics and physical properties of Kaffir lime leaf (*Citrus hystrix* DC). *Biomass Convers. Biorefinery* **2024**, *14*, 5601–5610.
25. Pradechboon, T.; Ramaraj, R.; Dussadee, N.; Chindaraksa, S. Advances application of a newly developed microwave rotary dryer for drying agricultural products of red chili pepper. *Biomass Convers. Biorefinery* **2024**, *14*, 9187–9196.
26. Ghasemkhani, H.; Khoshnam, F.; Kamandar, M.R. Drying apple slices in a rotating-tray convective dryer: A study on dehydration characteristics and qualitative attributes. *Iran. J. Chem. Eng.* **2021**, *18*, 16–32.
27. Jayaram, P.; Bhattu, N.R.; Jayaraman, J.; Nagappan, B.; Subramaniam, L.S. Experimental investigation on the treatment of mixed market waste by a novel rotary air dryer. *Waste Biomass Valorization* **2020**, *11*, 2153–2162.
28. Singh, P.; Mahanta, P.; Kalita, P. Experimental investigation of paddy drying characteristics in a slitless rotary fluidized-bed dryer. *Drying Technol.* **2022**, *40*, 3262–3272.
29. El-Mesery, H.S.; Qenawy, M.; Ali, M.; Hu, Z.; Adelusi, O.A.; Njobeh, P.B. Artificial intelligence as a tool for predicting the quality attributes of garlic (*Allium sativum* L.) slices during continuous infrared-assisted hot air drying. *J. Food Sci.* **2024**, *89*, 7693–7712.
30. Zadhosein, S.; Abbaspour-Gilandeh, Y.; Kaveh, M.; Szymanek, M.; Khalife, E.; Samuel, O.D.; Amiri, M.; Dziwulski, J. Exergy and energy analyses of microwave dryer for cantaloupe slice and prediction of thermodynamic parameters using ANN and ANFIS algorithms. *Energies* **2021**, *14*, 4838.
31. Ehiem, J.C.; Oduma, O.; Igbozulike, A.O.; Raghavan, V.G.; Aviara, N.A. Modeling the kinetics, energy consumption and shrinkage of avocado pear pulp during drying in a microwave assisted dryer. *Chem. Prod. Process Model.* **2024**, *19*, 879–889.
32. Sasikumar, R.; Mangang, I.B.; Vivek, K.; Jaiswal, A.K. Effect of ultrasound-assisted thin bed drying for retaining the quality of red bell pepper and compare the predictive ability of the mathematical model with artificial neural network. *J. Food Process Eng.* **2023**, *46*, e14468.
33. El-Mesery, H.S.; Ali, M.; Qenawy, M.; Adelusi, O.A. Application of artificial intelligence to predict energy consumption and thermal efficiency of hybrid convection-radiation dryer for garlic slices. *Eng. Appl. Artif. Intell.* **2024**, *138*, 109338.
34. Kaveh, M.; Zomorodi, S.; Szymanek, M.; Dziwulska-Hunek, A. Determination of drying characteristics and physicochemical properties of mint (*Mentha spicata* L.) leaves dried in refractance window. *Foods* **2024**, *13*, 2867.
35. Rashvand, M.; Nadimi, M.; Paliwal, J.; Zhang, H.; Feyissa, A.H. Effect of Pulsed Electric Field on the Drying Kinetics of Apple Slices during Vacuum-Assisted Microwave Drying: Experimental, Mathematical and Computational Intelligence Approaches. *Appl. Sci.* **2024**, *14*, 7861.
36. Huang, W.; Huang, D.; Chen, Y.; Gong, G.; Zhou, F.; Huang, S.; Auwal, M.; Li, L. Ultrasound-assisted medium-wave infrared drying performance of *Phyllanthus emblica* and artificial neural network modeling. *Int. Commun. Heat Mass Transf.* **2024**, *159*, 108028.
37. Tepe, T.K. Effect of pretreatments on drying characteristics, rehydration properties, and total energy consumption of carrot slices: Comparison between thin layer mathematical modelling and artificial neural network modelling. *Biomass Convers. Biorefinery* **2024**, *14*, 1373–1387.
38. AOAC. *Official Methods of Analysis of AOAC International*, 16th ed.; Association of Official Analytical Chemist International AOAC: Gaithersburg, MD, USA, 1997.
39. Huang, D.; Deng, R.; Auwal, M.; Wang, W.; Gong, G.; Li, L.; Sunden, B. Drying kinetics and energy consumption of astragalus membranaceus under infrared drying. *J. Therm. Sci. Eng. Appl.* **2024**, *16*, 071013.
40. Lemus-Mondaca, R.; Zura-Bravo, L.; Ah-Hen, K.; Di Scala, K. Effect of drying methods on drying kinetics, energy features, thermophysical and microstructural properties of *Stevia rebaudiana* leaves. *J. Sci. Food Agric.* **2021**, *101*, 6484–6495.
41. Motevali, A.; Minaei, S.; Banakar, A.; Ghobadian, B.; Khoshtaghaza, M.H. Comparison of energy parameters in various dryers. *Energy Convers. Manag.* **2014**, *87*, 711–725.
42. Kaveh, M.; Abbaspour-Gilandeh, Y.; Nowacka, M. Comparison of different drying techniques and their carbon emissions in green peas. *Chem. Eng. Process.-Process Intensif.* **2021**, *160*, 108274.

43. Geng, Z.; Wang, H.; Torki, M.; Beigi, M.; Zhu, L.; Huang, X.; Yang, X.; Hu, B. Thermodynamically analysis and optimization of potato drying in a combined infrared/convective dryer. *Case Stud. Therm. Eng.* **2023**, *42*, 102671.
44. Leilayi, M.; Arabhosseini, A.; Samimi Akhijahani, H.; Kaveh, M.; Nezamlou, N.; Aghaei, M. Energy and exergy efficiencies of batch paddy rice drying with liquefied petroleum gas dehumidification: A comprehensive analysis using adaptive neuro-fuzzy inference system and artificial neural networks approaches. *Energy Convers. Manag.* **2025**, *25*, 100826.
45. Meshkat, H.; Sharifian, F.; Hosainpour, A.; Nikbakht, A.M.; Kaveh, M. Analysis of energy and exergy of lavender extract powder in spray dryer. *Heat Transf.* **2024**, *53*, 4608–4624.
46. Icier, F.; Ozmen, D.; Cevik, M.; Cokgezme, O.F. Drying of licorice root by novel radiative methods. *J. Food Process. Preserv.* **2021**, *45*, e15214.
47. Dowlati, M.; Golpour, I.; Blanco-Marigorta, A.M.; Marcos, J.D.; de la Guardia, M.; Sheikhshoaei, H. A comprehensive assessment of energetic and exergetic performance for the dehumidification system of a processed pistachio production unit. *J. Food Process Eng.* **2023**, *46*, e14471.
48. Tezcan, D.; Sabancı, S.; Cevik, M.; Cokgezme, O.F.; Icier, F. Infrared drying of dill leaves: Drying characteristics, temperature distributions, performance analyses and colour changes. *Food Sci. Technol. Int.* **2021**, *27*, 32–45.
49. Cokgezme, O.F.; Gunes, N.C.; Bayana, D.; Icier, F. Life cycle assessment of a Photovoltaic-Assisted Daylight simulated dryer. *Sustain. Energy Technol. Assess.* **2024**, *65*, 103751.
50. Giang, N.T.N.; Tan, N.D.; Ha, H.T.N.; Van Thanh, D.; Van Khai, T.; Quyen, D.K. Artificial intelligence prediction the desirable moisture content of dried oyster mushroom (*Pleurotus sajor-caju*) for enhancing the cellulase-assisted extraction efficiency. *J. Agric. Food Res.* **2025**, *19*, 101561.
51. Camilo, M.O.; Carvalho, R.F.; Costa, A.B.; Junior, E.F.; Costa, A.O.; Sousa, R.C. Drying kinetic for moisture content prediction of peels Tahiti lemon (*Citrus latifolia*): Approach by machine learning and optimization-genetic algorithms and nonlinear programming. *S. Afr. J. Chem. Eng.* **2025**, *51*, 136–152.
52. Qenawy, M.; Ali, M.; El-Mesery, H.S.; Hu, Z. Analysis and control of hybrid convection-radiation drying systems toward energy saving strategy. *J. Food Sci.* **2024**, *89*, 9559–9576.
53. Abasi, S.; Minaei, S.; Khoshtaghaza, M.H. Effect of desiccant system on thin layer drying kinetics of corn. *J. Food Sci. Technol.* **2017**, *54*, 4397–4404.
54. Beigi, M.; Torki, M.; Khoshnam, F.; Tohidi, M. Thermodynamic and environmental analyses for paddy drying in a semi-industrial dryer. *J. Therm. Anal. Calorim.* **2021**, *146*, 393–401.
55. Zohrabi, S.; Seiiedlou, S.S.; Aghbashlo, M.; Scaar, H.; Mellmann, J. Enhancing the exergetic performance of a pilot-scale convective dryer by exhaust air recirculation. *Drying Technol.* **2020**, *38*, 518–533.
56. Ajetunmbi-Adeyeye, R.I.; Norazatul Hanim, M.R.; Maizura, M. Effects of superheated steam drying on the physical properties, functional characteristics, and antioxidant capacity of papaya powder. *J. Food Meas. Charact.* **2024**, *18*, 9086–9097.
57. El-Mesery, H.S.; Ashiagbor, K.; Hu, Z.; Alshaer, W.G. A novel infrared drying technique for processing of apple slices: Drying characteristics and quality attributes. *Case Stud. Therm. Eng.* **2023**, *52*, 103676.
58. Antal, T.; Páy, G.L.; Sikolya, L. Effect of Drying Methods on the Physical and Mechanical Properties of Dried Sweet Corn. In Proceedings of the International Multidisciplinary Conference, Nyíregyháza, Hungary, Baia Mare, Romania, 25–26 November 2021.
59. Aradwad, P.P.; Thirumani Venkatesh, A.K.; Mani, I. Infrared drying of apple (*Malus domestica*) slices: Effect on drying and color kinetics, texture, rehydration, and microstructure. *J. Food Process Eng.* **2023**, *46*, e14218.
60. Jafarifar, M.; Chayjan, R.A.; Dibagar, N.; Alaei, B. Modelling some engineering properties of walnut kernel undergoing different drying methods with microwave pre-treatment. *Qual. Assur. Saf. Crops Foods* **2017**, *9*, 463–478.
61. Liu, Z.L.; Bai, J.W.; Wang, S.X.; Meng, J.S.; Wang, H.; Yu, X.L.; Gao, Z.J.; Xiao, H.W. Prediction of energy and exergy of mushroom slices drying in hot air impingement dryer by artificial neural network. *Drying Technol.* **2020**, *38*, 1959–1970.
62. Tepe, T.K.; Tepe, F.B. Improvement of pear slices drying by pretreatments and microwave-assisted convective drying method: Drying characteristics, modeling of artificial neural network, principal component analysis of quality parameters. *J. Therm. Anal. Calorim.* **2024**, *149*, 7313–7328.
63. El-Mesery, H.S.; Qenawy, M.; Li, J.; El-Sharkawy, M.; Du, D. Predictive modeling of garlic quality in hybrid infrared-convective drying using artificial neural networks. *Food Bioprod. Process.* **2024**, *145*, 226–238.
64. Günaydın, S.; Ropelewska, E.; Sacilik, K.; Çetin, N. Exploration of machine learning models based on the image texture of dried carrot slices for classification. *J. Food Compos. Anal.* **2024**, *129*, 106063.

65. Parida, C.; Sahoo, P.K.; Nasir, R.; Waseem, L.A.; Tariq, A.; Aslam, M.; Hatamleh, W.A. Exergy assessment of infrared assisted air impingement dryer using response surface methodology, Back Propagation-Artificial Neural Network, and multi-objective genetic algorithm. *Case Stud. Therm. Eng.* **2024**, *53*, 103936.
66. Omari, A.; Behroozi-Khazaei, N.; Sharifian, F. Drying kinetic and artificial neural network modeling of mushroom drying process in microwave-hot air dryer. *J. Food Process Eng.* **2018**, *41*, e12849.
67. Aghbashlo, M.; Hosseinpour, S.; Mujumdar, A.S. Application of artificial neural networks (ANNs) in drying technology: A comprehensive review. *Drying Technol.* **2015**, *33*, 1397–1462.

**Disclaimer/Publisher's Note:** The statements, opinions and data contained in all publications are solely those of the individual author(s) and contributor(s) and not of MDPI and/or the editor(s). MDPI and/or the editor(s) disclaim responsibility for any injury to people or property resulting from any ideas, methods, instructions or products referred to in the content.